

https://dspace.org/

Estimating water loss from the Renoster River, Free State province, South Africa

Brown, Fred Herman

2006-11-17T08:04:59Z
http://hdl.handle.net/10539/1831

Downloaded from a DSpace repository. https://dspace.org/

ESTIMATING WATER LOSS FROM THE RENOSTER RIVER, FREE STATE PROVINCE, SOUTH AFRICA

Fred Herman Brown

A research report submitted to the Faculty of Engineering and the Built Environment, University of the Witwatersrand, Johannesburg, in partial fulfillment of the requirements for the degree of Master of Science in Engineering

Johannesburg 2005

DECLARATION

I declare that this research report is my own, unaided work. It is being submitted for the Degree of Master of Science in the University of the Witwatersrand, Johannesburg. It has not been submitted previously for any degree or examination in any other University.

_____

1st day of June, 2005

ABSTRACT

The Renoster River is a minor left-bank tributary of the Vaal River located some 120 km south-west of Johannesburg in the Free State Province of South Africa. The river is dammed by the Koppies Dam, which divides the river into upper and lower basins. No water is released directly from the Koppies Dam into the Renoster River channel except as a protective measure during natural flooding events. Irrigation releases are made through a separate canal system.

The lower Renoster River was modeled as a series of channels, crossing four quaternary catchments. Hydraulic routing was used to estimate potential flow losses for discrete flow events. Out-of-bank flow was found to occur when flow exceeded 300 m^3/s. A Pitman monthly rainfall-runoff hydrologic model was used to model longer term historical streamflow data and associated losses.

Flow losses for individual flood events along the lower Renoster River were found to vary between 3% and 17%. For a longer term constant flow regime, losses can be expected to range between 10% and 40%. Based on both the hydraulic and hydrologic models, the primary cause of flow loss was found to be evaporation, with insignificant transpiration and transmission losses.

For eighty years flow in the lower Renoster River has been artificially controlled. Within that time period the river has adjusted itself to the imposed anthropogenic flow regime. Water losses associated with planned releases into the lower Renoster River can be minimized by using a high discharge rate, to a maximum of 300 m^3/s, combined with larger volumetric flows. Evaporation losses can be significant, and release strategies will need to take this into consideration.

ACKNOWLEDGEMENTS

The author would like to thank family, friends and colleagues for their support, encouragement and assistance. Thanks also to Professor Chris James, who tolerated with grace and patience the sometimes absurd opinions of an amateur. Thanks also to my wife, who still seems to think this is a good idea, and finally, last but not least, many thanks to my son Mitchel, field assistant extraordinaire!

TABLE OF CONTENTS

DECLARATION i

ABSTRACT ii

ACKNOWLEDGEMENTS iii

TABLE OF CONTENTS iv

LIST OF FIGURES vi

LIST OF TABLES vii

LIST OF SYMBOLS AND ACRONYMS viii

1 INTRODUCTION 1

1.1 Purpose of this study 1
1.2 Data sources 3
1.3 Approach followed 3

2 THE RENOSTER RIVER BASIN 4

2.1 Study area 4
2.2 Basin characteristics 4
2.2.1 General features 4
2.2.2 Koppies Dam release flows 13
2.2.3 The lower Renoster River basin 14
2.2.4 Drainage network 15
2.3 River classification 18
2.3.1 Hierarchical systems 18
2.3.2 Representative reaches 20

3 HYDRAULIC MODEL 23

3.1 Water balance 23
3.2 Muskingum flow routing 28
3.2.1 Theory 28
3.2.2 Muskingum routing hydrographs 29
3.3 Kinematic wave routing 33
3.3.1 Theory 33
3.3.2 Manning's Coefficient 34
3.3.3 Kinematic wave routing hydrographs 34
3.3.4 Loss calibration 38
3.4 Theoretical losses 39

4 HYDROLOGICAL MODEL 41

4.1 Pitman runoff model 41
4.1.2 Default Pitman model parameters 43
4.2 WRSM2000 model 43
4.2.1 Model requirements 43
4.2.2 Model implementation 44
4.2.3 Calibration 46
4.4 Model results 46
4.4.1 Parameter set 46
4.4.2 Theoretical losses 49

5 SUMMARY 50

REFERENCES 52

LIST OF FIGURES

Figure 1: The Renoster River basin. 2
Figure 2: Digital Elevation Model of the Renoster River. 6
Figure 3: Quaternary catchments of the lower Renoster River basin. 7
Figure 4: Gauging stations in the lower Renoster River basin. 8
Figure 5: Selected SAWS rainfall stations. 9
Figure 6: Hydrograph and isoheytal map January 1985. 10
Figure 7: Blue stream topographic network. 12
Figure 8: Flow Duration Curve for the lower Renoster River – Koppies Dam daily release rate. 13
Figure 9: 3rd, 4th, 5th and 6th order transitions for the Renoster River. 16
Figure 10: Renoster River stream order. 17
Figure 11: Longitudinal profile of the Renoster River. 17
Figure 12: Representative reaches along the lower Renoster River. 22
Figure 13: Perennial pools along the lower Renoster River. 26
Figure 14: Retention weir and Gauging Station C7H001. 27
Figure 15: Hydrograph and Muskingum routing Koppies release January 1984. 30
Figure 16: Hydrographs and Muskingum routing Koppies release November 1987. 31
Figure 17: Hydrographs and Muskingum routing Koppies release January 1988. 32
Figure 18: Kinematic wave routing model implementation. 36
Figure 19: Kinematic wave hydrographs. 37
Figure 20: Stage/Discharge rating curve for the lower Renoster River macro-channel. 39
Figure 21: Pitman runoff model flow chart. 42
Figure 22: Lower Renoster River basin model network. 45
Figure 23: Calibration of the basin model – monthly simulated and observed flows. 48
Figure 24: Calibrated monthly hydrograph. 48
Figure 25: Simulated water loss in the lower Renoster River. 49

LIST OF TABLES

Table 1: Hydrological data sources and periods covered. 3
Table 2: Catchment characteristics. 14
Table 3: South African geomorphological hierarchical classification system. 19
Table 4: Reach hierarchical classification system. 20
Table 5: Representative reaches. 21
Table 6: Perennial pool volumes and extent of riparian vegetation. 25
Table 7: Muskingum flow routing results. 29
Table 8: Estimated Manning's roughness coefficients. 34
Table 9: Calibrated Manning's roughness coefficients. 35
Table 10: Estimated travel time per catchment 38
Table 11: Estimated percent evaporation losses per reach. 38
Table 12. Theoretical water losses as a percentage of total release. 40
Table 13: Pitman model parameters. 42
Table 14: Regionalised catchment model parameters. 43
Table 15: Model parameter set. 47
Table 16: Simulation summary statistics (Route 17 output). 47

LIST OF SYMBOLS AND ACRONYMS

SYMBOL	EXPLANATION
A	Cross-sectional area
AMSL	Above Mean Sea Level
DEM	Digital Elevation Model
dS/dT	Rate of change of channel storage
E	Evapotranspiration
FT	Pitman runoff when ST is reached
GL	Pitman soil moisture runoff lag
GW	Pitman maximum groundwater runoff
I	Inflow
K	Muskingum storage time
MAE	Mean Annual Evaporation (mm/a)
MAR	Mean Annual Runoff (mm/a)
n	Manning's roughness coefficient
O	Outflow
P	Precipitation
PI	Pitman interception storage
POW	Pitman power of soil-moisture runoff equation
Q	Flow discharge (m^3/s)
R	Wetted perimeter
R	Pitman evaporation – soil moisture relationship
S_0	Gravity force term
S_f	Friction force term
SL	Pitman soil moisture storage below which no runoff occurs
ST	Pitman subsurface storage
T	Transmission loss
TL	Pitman surface runoff lag
x	Muskingum weighting factor
ZMAX	Pitman maximum catchment absorption rate
ZMIN	Pitman minimum catchment absorption rate

1 INTRODUCTION

The Renoster River is a minor left-bank tributary of the Vaal River located some 120 km south-west of Johannesburg in the Free State Province of South Africa (Figure 1). The river, with a total basin area of approximately 6200 km^2, flows from east-to-west along the southern flanks of the Vredefort Dome, a prominent meteoroid impact structure dating ~2.02 Ga (Bootsman and Reimold, 2001). The river was dammed in 1925 by the Koppies Dam, which divides the river into upper and lower basins.

No water is released directly from Koppies Dam into the Renoster River channel except during natural flooding events. Irrigation releases are made through a separate canal system. During the wet summer months the river experiences occasional turbid flow and during the dry summer months the river is reduced to a series of perennial pools. Several weirs and numerous small earth dams within the Renoster River basin reduce the amount of runoff available, and stream habitat has been modified to such an extent that there are effectively no stones in current. Due to the extensive anthropogenic alteration overall river health is considered poor (River Health Program, 2003).

1.1 Purpose of this study

Water retained by the Koppies Dam reservoir could potentially be utilized for purposes other than agriculture, such as small scale mining (Alheit and Wiid, 2003). However, no estimates are available on the potential loss of water released through the Renoster River from the Koppies Dam to a downstream site, a parameter required by the planning engineer for costing purposes. The purpose of this study is to provide preliminary estimates of the potential water loss in a format usable at the conceptual and pre-feasibility project stage. Water losses are expressed as a lumped parameter in terms of percentage loss of total release, in order to allow for a preliminary estimate of total release requirements for costing purposes. Longer term hydrologic processes are modeled as input parameters within a semi-distributed system and calibrated against existing streamflow data, allowing a variety of flow regimes to be simulated and potential losses estimated.

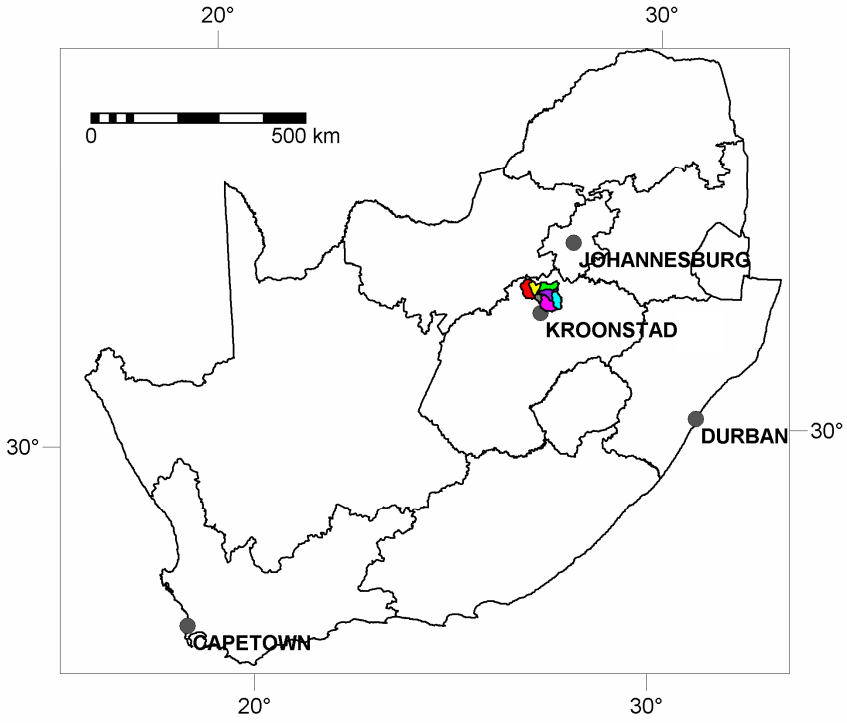


Figure 1: The Renoster River basin and quaternary catchments.

1.2 Data sources

Data used for this study were drawn from several sources. Topographic information was derived from the South African 1:50000 digital topographical data sets (Chief Directorate, Surveys and Mapping, 1994). River channel geometry and cross sections were mapped during the period November 2004 – January 2005. Daily rainfall data were extracted from Lynch (2003), and daily streamflow data were downloaded from the Department of Water Affairs and Forestry database (DWAF, 2004). Monthly naturalized streamflow data and monthly rainfall data are from Midgley et al. (1994).

The hydrological data available cover a number of periods (Table 1). In order to provide consistency in the information used, the data for this study were limited in general to the period 1978 – 1988, which overlapped the various sources. Periods referred to represent the hydrological year, from October to September.

Table 1: Hydrological data sources and periods covered.

	PERIOD				
Gauge:	***C7R001***	***C7H005***	***C7H006***	***C7H003***	***C7H001***
Daily Discharge (m^3/s) [1]	1978 – 1989	1954 – 1994	1978 – 2004	1947 – 1987	----
Monthly Naturalized Streamflow (m^3/month)[2]	1920 – 1988	----	1977 – 1989	1947 – 1989	1923 – 1947
Daily Rainfall (mm)[3]	1900 – 2000				
Monthly Rainfall (% MAP)[2]	1920 – 1988				

[1]DWAF 2004.
[2]Midgley et al. 1994
[3]Lynch 2003.

1.3 Approach followed

Water losses for the lower Renoster River were modeled using both a hydraulic and a hydrological approach.

Hydraulic models were used to estimate instantaneous water loss from discrete events, based on measured input and output hydrographs. Data from the hydrographs were used to calibrate a Muskingum routing model as well as a kinematic wave model, and short term losses simulated using the calibration parameters derived from both models.

Longer term water losses were estimated using a semi-distributed Pitman-type rainfall/runoff model, calibrated against measured output hydrographs. Total losses were then modeled using the derived rainfall/runoff relationship for a monthly time step.

2 THE RENOSTER RIVER BASIN

In order to establish realistic parameters for the hydraulic and hydrological models, the geological and hydrological characteristics of the Renoster basin were established from a combination of literature sources, field work and a digital elevation model. This was combined with geographic information relating to quaternary basins, gauging stations and rainfall locations into a geographical information system database using the ILWIS 3.2 Academic © software package (van Westen and Farifteh 2002). All derived information was thus available in a standard format for analysis.

2.1 Study area

In order to establish basic hydraulic and hydrologic model parameters such as channel geometry, slope and chainage, a digital elevation model (DEM) was created using the South African 1:50000 digital topographical data sets (Chief Directorate, Surveys and Mapping, 1994). The study area selected is 125 km by 112 km and includes the entire Renoster River basin (Figure 2). The lower Renoster River basin has been subdivided by Midgley et al. (1994) into seven quaternary catchments (C70D, C70E, C70F, C70H, C70J and C70K) – Figure 3. Three gauging stations have been erected along the lower Renoster River. Gauge C7R001 measures discharge from the Koppies Dam twenty metres below the spillway. Gauge C7H001 is associated with a retention weir constructed in the early 1920's. Gauge C7H005 was used prior to construction of the Koppies Dam, and gauge C7H006 has been in use consistently from 1978 to the present. Catchment C70K, which contains the lower Renoster River between Station C7H006 and its confluence with the Vaal River is ungauged. Within the lower Renoster River basin only the Heunigspruit (C70G) is separately gauged (C7H003) from the Renoster River itself (Figure 4).

2.2 Basin characteristics

2.2.1 General features

Relief in the study area ranges between ~1100 m AMSL and ~1700 m AMSL. In Figure 2 three geomorphic domains can be identified: a desiccated eastern highlands, a flat lying western floodplain, and the Vredefort Dome. The Renoster River cuts across all three domains, draining the eastern highland, crossing the southern flank of the Vredefort Dome, and flowing into the western floodplain.

The Renoster River basin lies in the summer rainfall zone of Southern Africa, and receives approximately 70% of annual rainfall during the hydrological summer months of October to

March. The remaining 30% is associated with isolated showers and thunder storms during the cooler months of April to September. Mean Annual Precipitation (MAP) is 589 mm. Daily precipitation data are available from a number of South African Weather Services rainfall stations within and adjacent to the Renoster River basin (Figure 5). Although not all the data are equally reliable (Lynch, 2003), isohyets do demonstrate that both rainfall and rainfall response can vary across the basin during a single storm event across the basin. An isohyetal map was generated from SAWS data for such an event using inverse distance estimation over a 25m x 25m regularized grid. (Figure 6). The results demonstrate that rainfall/response will vary across the basin in response to precipitation differences.

Gross Mean Annual Evaporation (MAE) varies from 1600 mm to 1690 mm, averaging 1670 mm/a. Maximum potential evaporation occurs in January. Average wind speed and direction were obtained for the Kroonstad weather station (SAWS 0365398) 50 km south of the study area, indicating mild easterly prevailing winds with an average speed of 4 m/s.

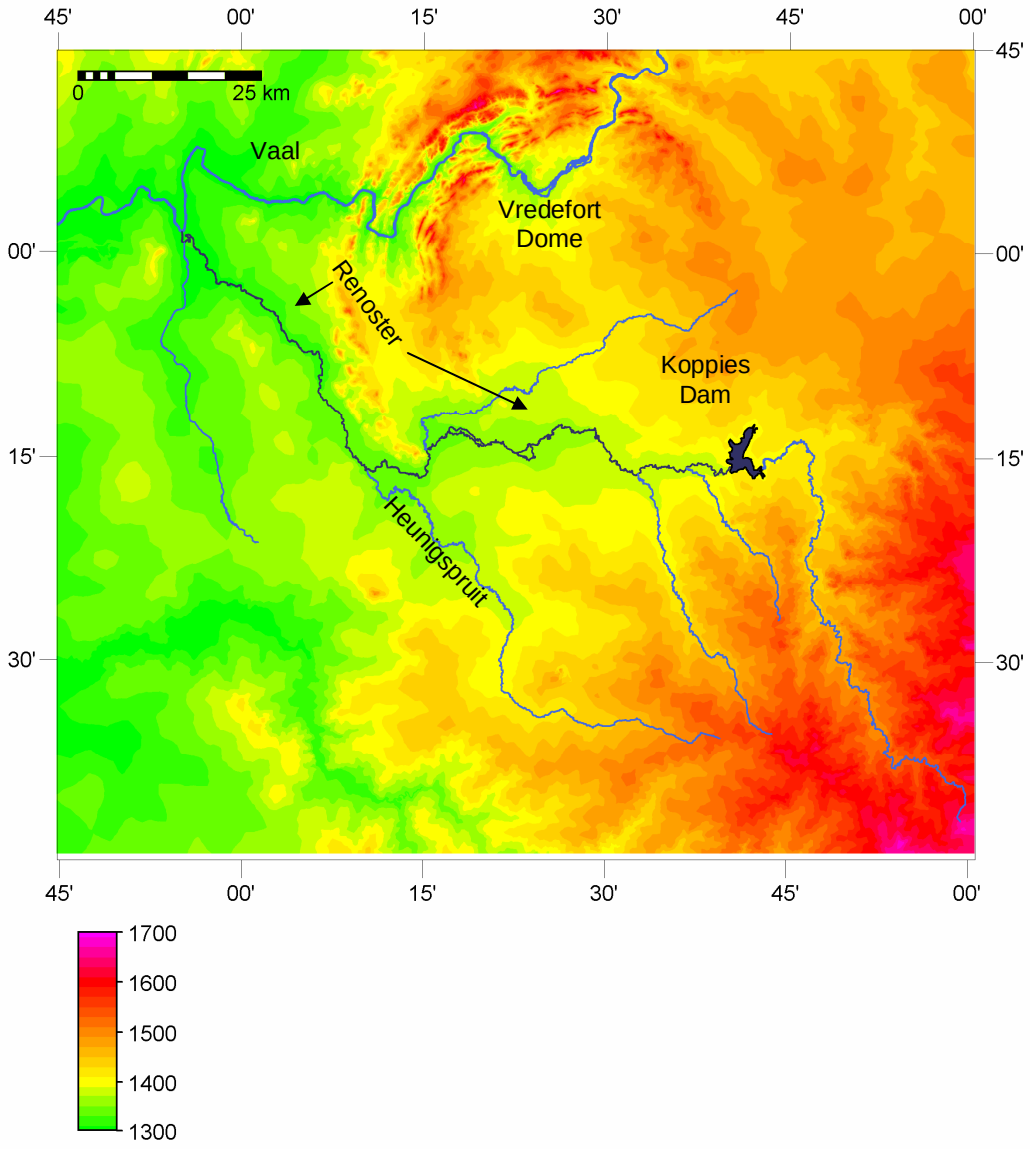


Figure 2: Digital Elevation Model of the Renoster River.
Elevation in metres above sea level.

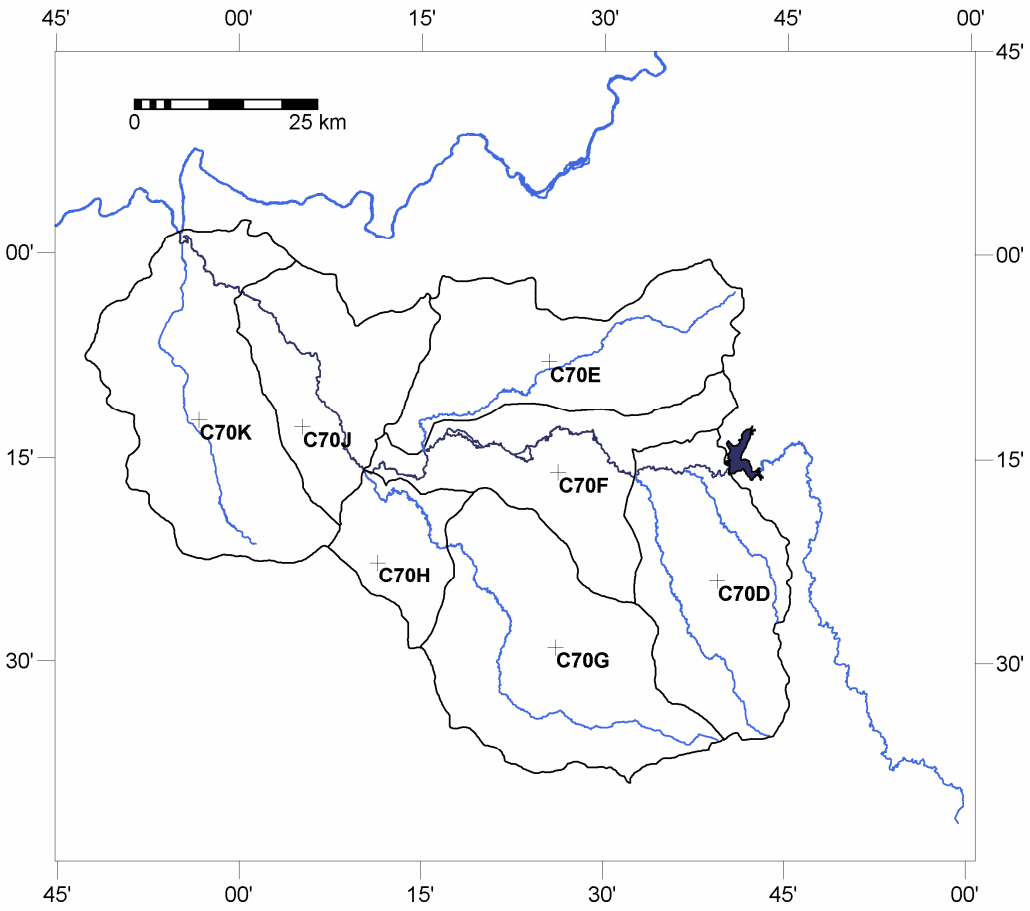


Figure 3: Quaternary catchments of the lower Renoster River basin.

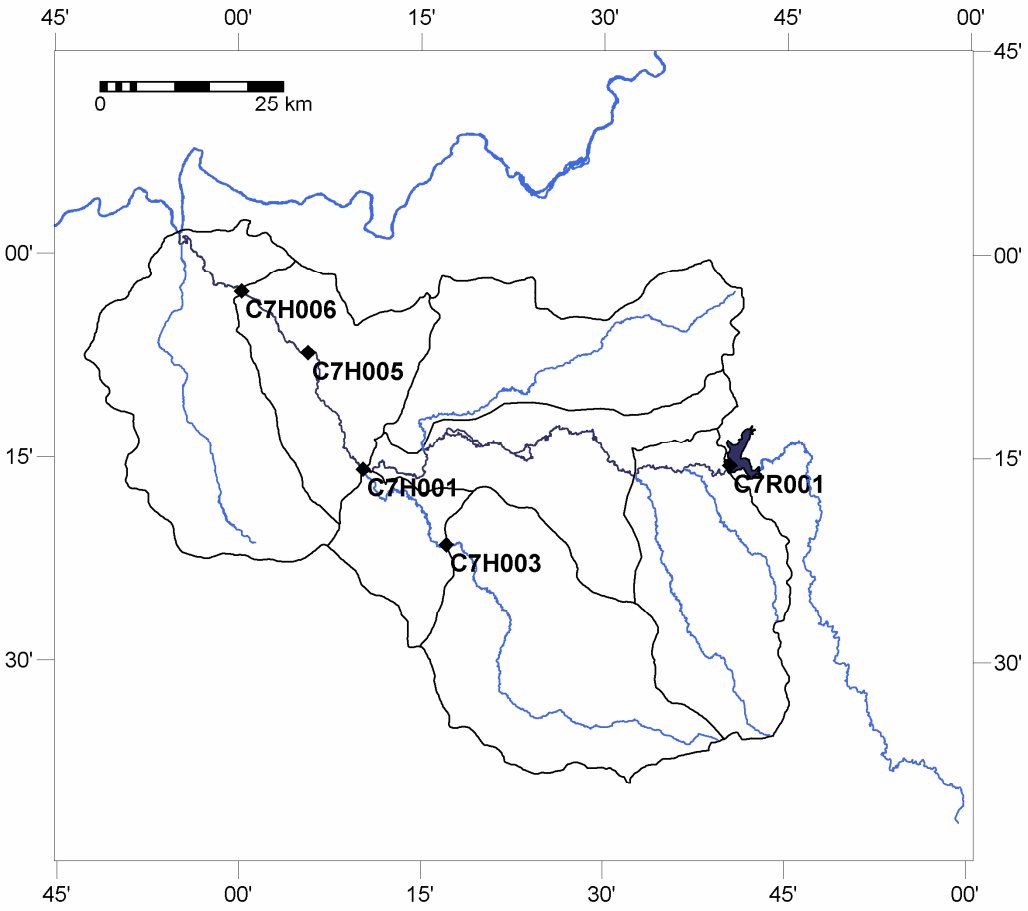


Figure 4: Gauging stations in the lower Renoster River basin.

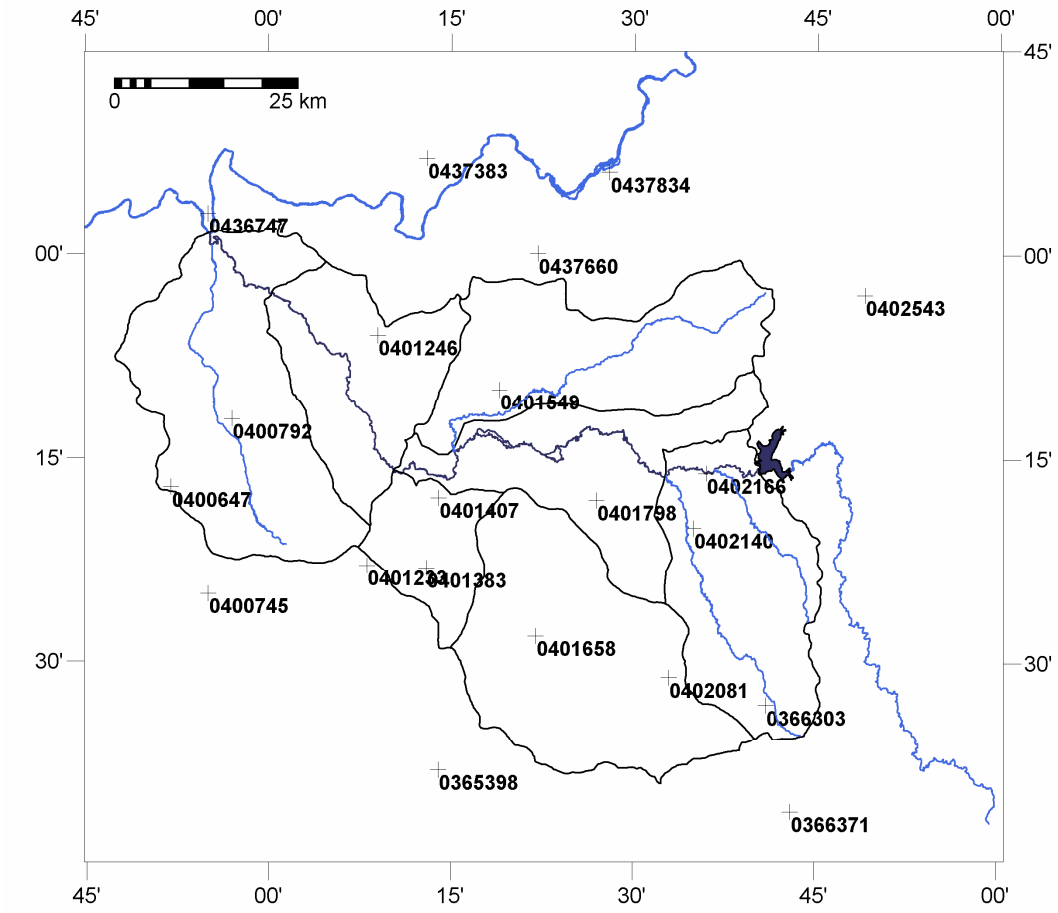


Figure 5: Selected SAWS rainfall stations.

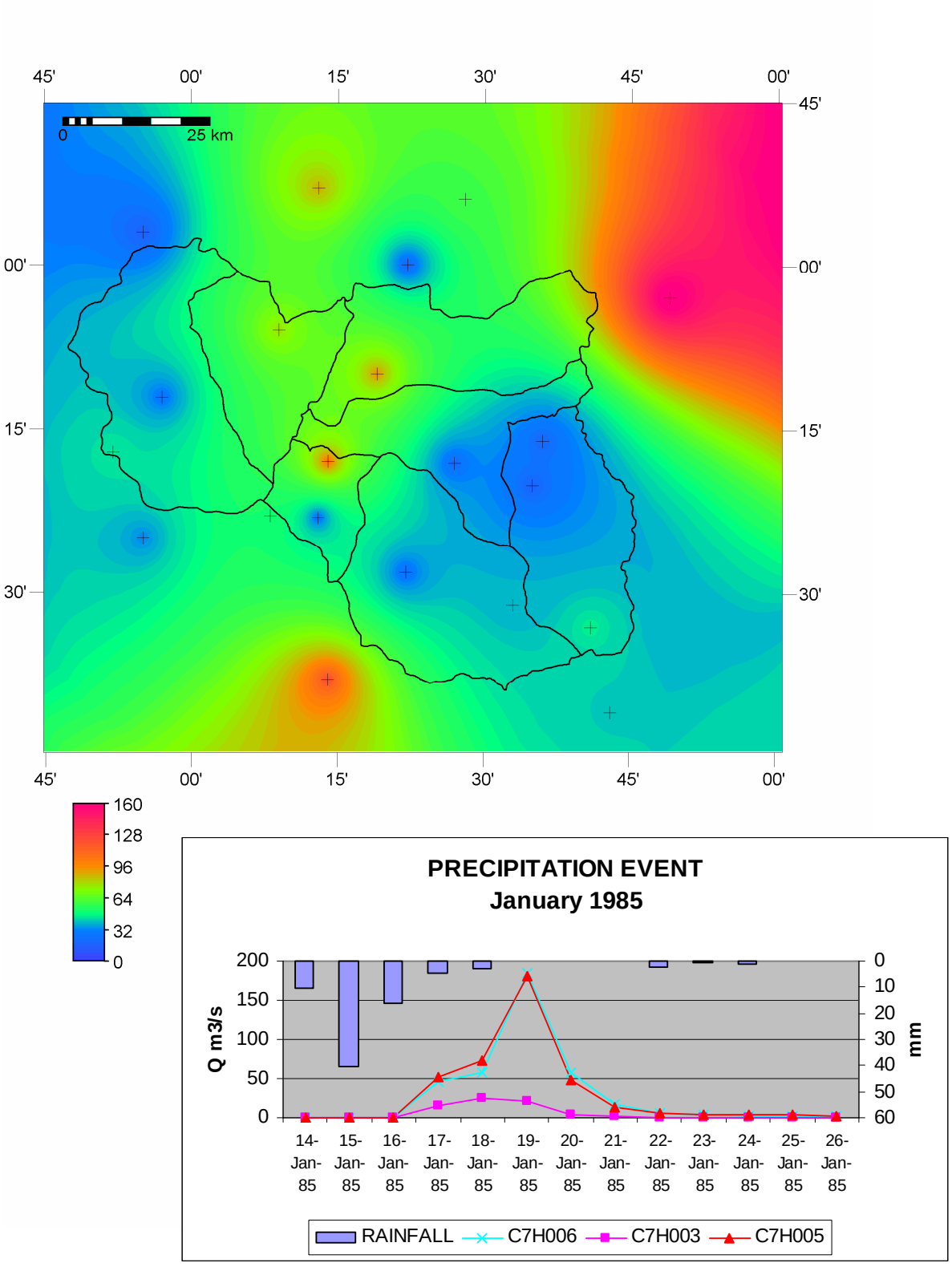


Figure 6: Hydrograph and isoheytal map January 1985.
Inverse squared distance estimate of total rainfall for the period 14 – 26 January 1985. Isohyets in mm. Grid size = 25 x 25 m; local station effects are apparent due to coarse data resolution.

The blue-line topographic stream network coincident to the Renoster River basin displays a marked annular/radial drainage pattern due to the geological controls associated with the Vredefort Dome meteoroid impact structure (Figure 7). Lower order streams are radial away from the central uplift associated with the Vredefort event, with subsidiary streams joining at right angles along fold axes. Annular flows adjacent to the dome are also controlled by the lithological contrasts of sharply upturned strata, which alternate between resistant quartzite ridges and less resistant shale formations (Bootsman and Reimold, 2001). Exceptions are the Vaal River to the north, a superimposed river system that exploits radial faulting associated with the impact structure, and the Renoster River system to the south, which flows parallel to pre-impact Achaean deformation structures (Gibson et al., 2002).

The area has been classified as Dry Clay Highveld Grassland in the east, grading into Moist Cool Highveld Grassland towards the west (Low and Rebelo, 1996). Dry clayey duplex soils predominate, and land use is primarily small scale agriculture. Approximately 60% of land use in the basin comprises natural grassland which is utilized for cattle grazing, with the remainder given over to dryland cultivated crops, predominately maize and wheat. Water bodies and urban development compromise less than 1% of the total basin (River Health Program, 2003).

The local geology consists of overturned and folded Archean basement granites and gneisses associated with the outcropping Vredefort Dome structure to the north, overlain by encroaching thick Karoo cover in the south (Bootsman and Reimold, 2001). Small scale mining in the area has historically included diamonds, coal, bentonite, limestone, dimension stone and stone aggregate, although no formal mining operations are currently taking place.

The Koppies Dam restricts sediment supply from the upper reaches of the Renoster River, creating a sediment-starved network downstream (Rowntree and Wadeson, 1999). This has resulted in a channel form dominated by lateral erosion and channel widening, degradation and slow downcutting of the bed with little associated change in gradient, characteristic of long-term river development in an arid environment downstream of a dam (Graf, 1988). Erosion of the bed and banks will continue as long as sediment movement thresholds are within the flow capacity, although the effects of erosion are considered minor in resistant bedrock channels (Rowntree and du Plessis, 2003).

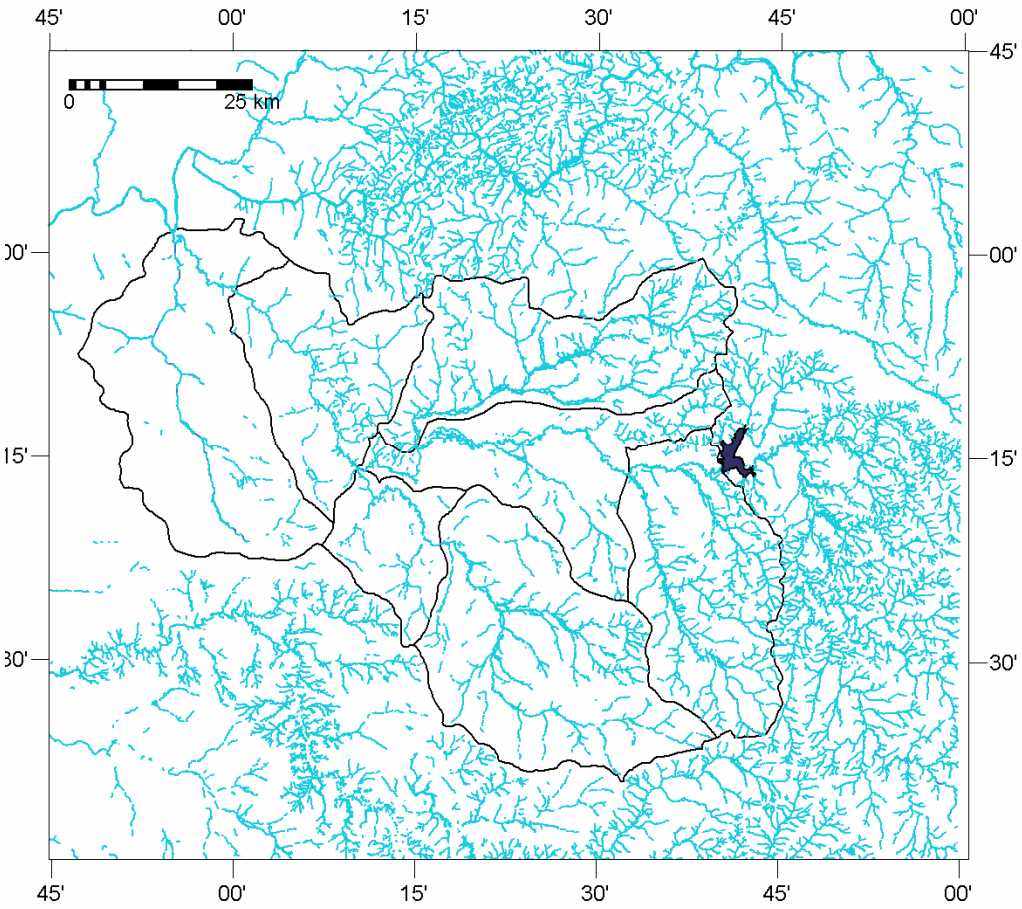


Figure 7: Blue stream topographic network.
Chief Directorate, Surveys and Mapping (1994).

2.2.2 Koppies Dam release flows

Koppies Dam is a 2.4 km long gravity/earth-fill combination structure (Midgley et al., 1994). The original dam was raised in 1971 to its current height of twenty-five metres in order to offset siltation and ensure better utilization of available water supplies (Turton et al., 2004). The dam has a current capacity of between ~ 41 million m^3 (Midgley et al., 1994) and ~ 47 million m^3 (River Health Program, 2003). Because water is only released from the Koppies Dam during natural flooding events, flow conditions in the lower Renoster River are predominately the result of human activity.

Using daily flow data from CTR001 over the period 1978 – 1988, a Flow Duration Curve (FDC) was generated for the lower Renoster River based on the inverse normal distribution function available with standard Microsoft Excel™ spreadsheets (Figure 8). Daily flow data show a wide variance in release rates, ranging from a maximum of 571 m^3/s to a low of 0.01 m^3/s, with an average of 2.5 m^3/s.

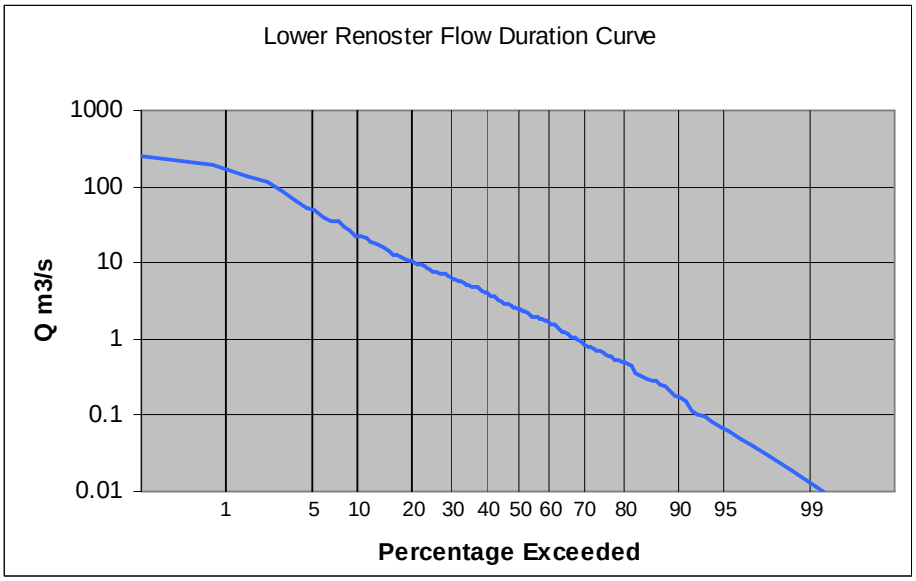


Figure 8: Flow Duration Curve for the lower Renoster River – Koppies Dam daily release rate.

2.2.3 The lower Renoster River basin

The lower Renoster River crosses the C70D, C70F, C70J and C70K quaternary catchments (Figure 3), draining a total area of 3997 km^2. From its confluence with the Vaal River up to the Koppies Dam the total river chainage is ~144 km. The longitudinal profile is gentle and concave, with no major break in slope below the Koppies Dam (Figure 4). Overall sinuosity (defined as the ratio between macro-channel length to valley length) is ~1.6, varying between 1.3 and 1.9. The Renoster River changes from a cross-cutting superimposed river flowing east-to-west to an annular system flowing southeast-to-northwest in the vicinity of the Heunigspruit confluence. Where open to inspection the river appears to be scoured down to bedrock along its entire course.

The lower Renoster River basin encompasses a number of geomorphic domains. Quaternary catchments C70D and C70G drain the desiccated eastern highlands. Catchment C70E drains the central Vredefort Dome structure. Catchments C70H and C70J occupy the western floodplains, and catchment C70K cross-cuts several resistant quartzite structures to link with the Vaal River.

Table 2: Catchment characteristics.

Catchment[1]	Area[2] (km^2)	Chainage[3] (km)	Slope[4] (m:m)	MAE[5] (mm)	MAP[6] (mm)	Irrig. Area[7] (km^2)	Order[8]
C70D	675	21.2	0.0013	1600	586	2.2	4
C70E	693	81.8	0.0020	1630	578	2.3	4
C70F	564	66.9	0.0007	1620	574	1.8	6
C70G	901	115.0	0.0016	1600	577	2.9	4
C70H	251	34.4	0.0006	1650	568	0.8	4
C70J	521	37.8	0.0012	1670	575	1.7	6
C70K	392	18.3	0.0007	1690	565	2.9	3
LOWER RENOSTER	3997	144.2	0.0077	1610	589	14.6	6

[1,2,5,6,7] Midgley et al. (1994).
[3]True river distance from 1:50000 digital topographic data set.
[4]S1085 slope along principle drainage.
[5]Gross Mean Annual Evaporation (S-Pan).
[6]Annual Mean Average Precipitation.
[8] Horton-Strahler.

2.2.4 Drainage network

A drainage network can be defined as a system of connected channels within a basin. A catchment is an area that contributes water and sediment to the drainage network. The relative geometry of the channels and catchments can be described by assigning a numerical stream order to the system components. Assuming a dendritic network with no triple junctions, stream order can be allocated using the following rules, based on the Horton-Strahler approach (Knighton, 1998).

1. fingertip tributaries originating at source are designated order 1;
2. the junction of two streams of order n forms a downstream segment of order n + 1;
3. the junction of two streams of unequal order forms a segment equal to the higher order.

The Horton-Strahler approach was utilized with the 1:50000 blue-line topographic stream network to classify the Renoster River basin. The Renoster River basin as a whole corresponds to a 6^{th} order drainage network (Figure 9). The relationship between stream order and stream number (the number of stream segments of a particular order) was found to be approximately geometric (Figure 10), which is typical of a branching network system and provides a crude index of basin physical processes.

No significant order changes occur within the lower Renoster River basin, suggesting that the tributaries make an insignificant contribution to the flow regime, and that no significant change in the physical processes occurs due to tributary inflow along the course of the lower Renoster River.

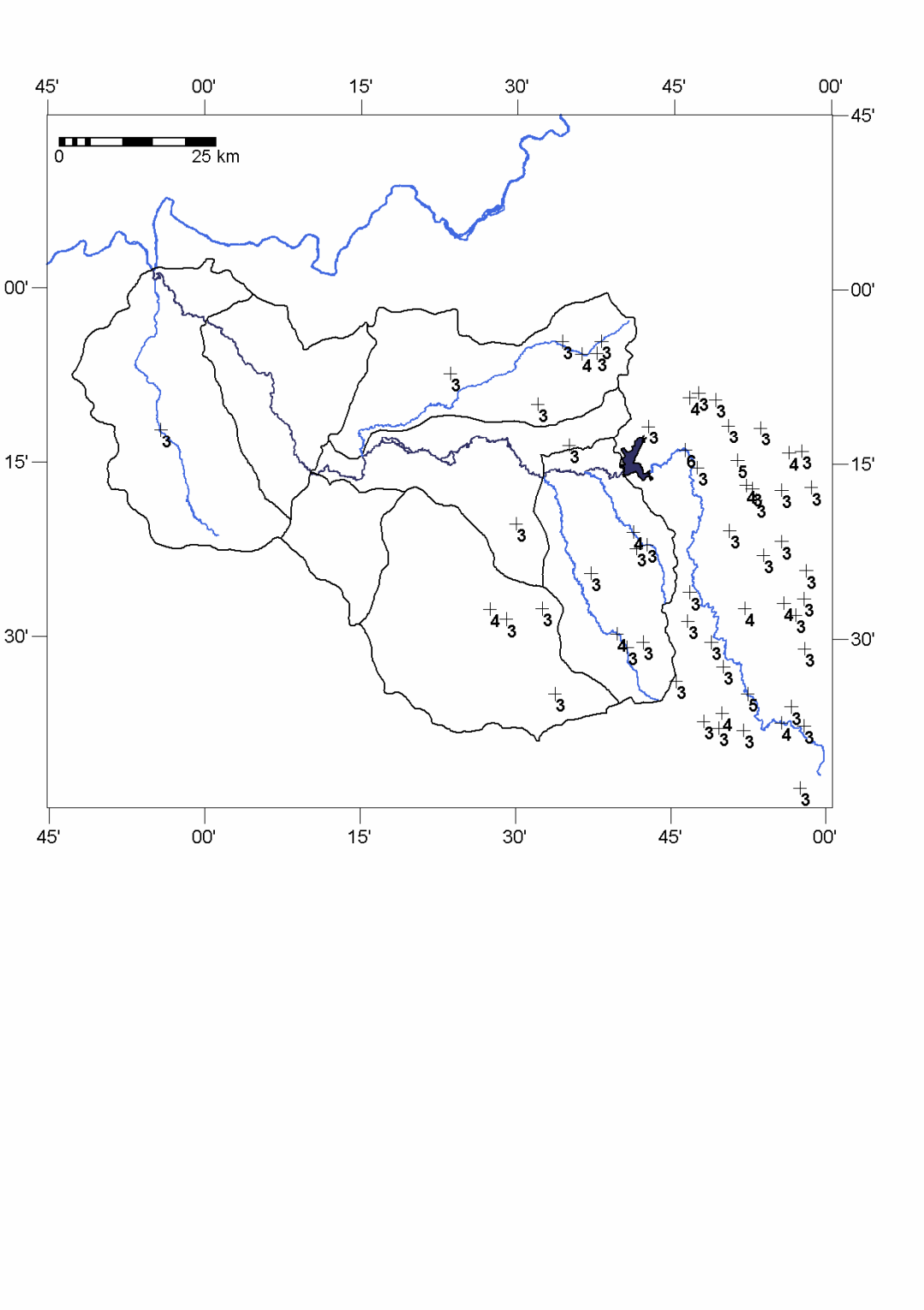


Figure 9: 3rd, 4th, 5th and 6th order transitions for the Renoster River.

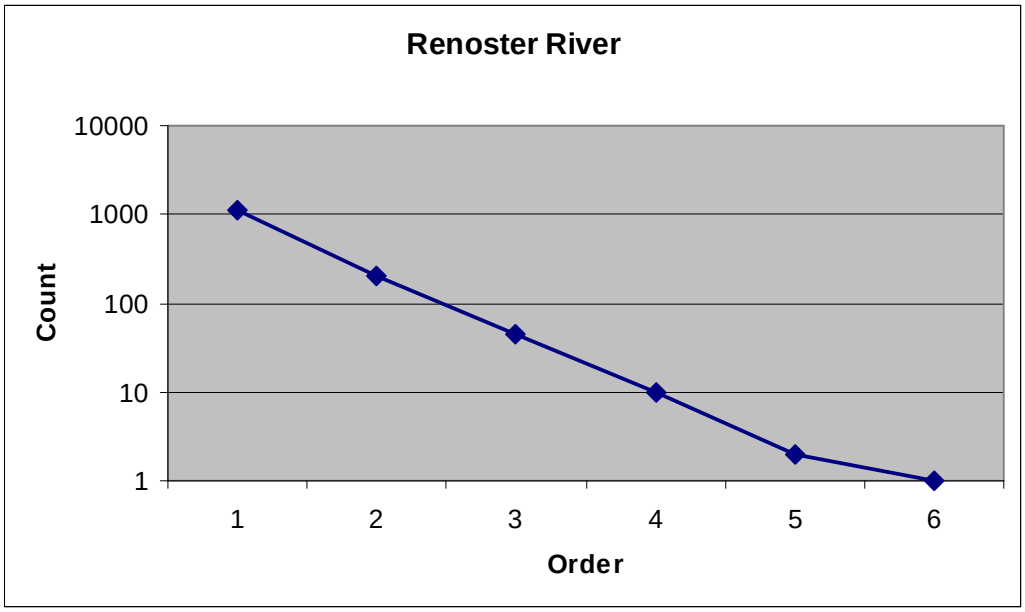


Figure 10: Renoster River stream order.

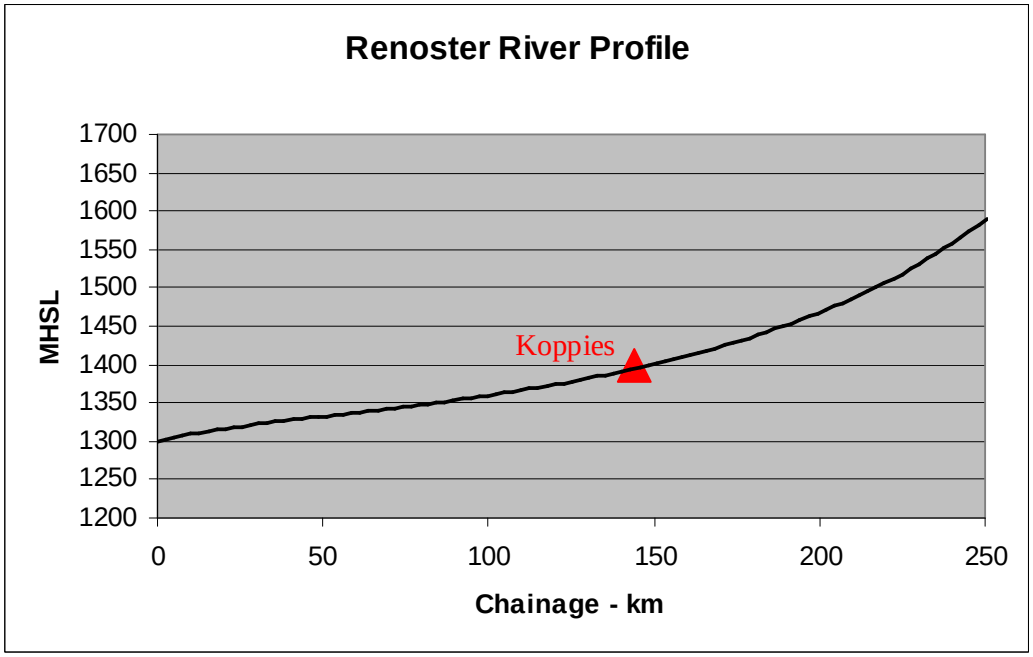


Figure 11: Longitudinal profile of the Renoster River.

2.3 River classification

Classification allows for the comparison of fluvial systems, their geomorphic and hydraulic parameters, as well as the modeling of their responses to changes in boundary conditions. It further allows linkages between catchments and channels to be modeled over a range of spatial scales (Rowntree and Wadeson, 1999), and facilitates the analysis of poorly known segments based on experience and knowledge of similar systems.

By identifying and classifying the various sections of the lower Renoster River into reaches, based on their distinctive geological, hydrological, sedimentological and vegetational attributes, parameters can be selected that effectively represent the actual physical systems at work. In addition, model parameters can then be extended to other reaches that are physically similar, allowing for extrapolation in data poor sections of the river.

2.3.1 Hierarchical systems

Several classification systems are available for use in South Africa for the classification of drainage networks. Lerner (2003) classified rivers by their flow characteristics (perennial, seasonal or ephemeral) and vertical position relative to the water table (perched, intermittent or connected) – thus the Renoster River might be considered a seasonal perched river in this system. Xu et al. (2002) has expanded this scheme for use in South Africa, by specifying classification criteria for the upper, middle and lower stream courses.

The simplest hierarchical system in general use in South Africa is the WR90 system of Midgley et al. (1994), which divides Southern Africa into 22 primary drainage regions, subdivided into secondary and tertiary regions and quaternary catchments. The 1946 defined quaternary catchments are demarcated by watershed boundaries, subsidiary streams and historical stream gauging sites. In this system the lower Renoster River basin lies in drainage region C, primary basin 7, and encompasses seven quaternary catchments.

Other river classification schemes have been developed to specifically address Southern African climatic conditions, and are typically based primarily on geomorphologic (e.g. Rowntree and Wadeson, 1999) or hydraulic parameters (e.g. Heritage et al., 2000) at a number of scales.

The South African Hierarchical System proposed by Rowntree and Wadeson (1999) is based on two distinct sets of geomorphologic parameters: areal features related to the catchment, and channel features which constitute the drainage network. Within this system six levels are

recognized: c*atchment, zone, segment, reach, unit* and *biotope*. Simplified definitions for each level are given in Table 3 below.

Table 3: South African geomorphological hierarchical classification system.
After Rowntree and Wadeson (1999).

LEVEL	**DESCRIPTION**	**TYPICAL SCALE**
Catchment	Land surface contributing water and sediment to a river network.	km+
Zone	Area within a catchment which is homogenous with respect to flood runoff and sediment production.	km+
Segment	Length of channel along which there is no significant change in discharge or sediment load.	km+
Reach	A length of channel with a characteristic channel pattern, degree of incision and assemblage of channel morphologies.	km
Unit	Individual morphological units.	m - km
Biotope	Habitat assemblage	m

The representative reach hierarchical classification system of Heritage et al. (2000), although superficially similar, is more directly concerned with the characterization of hydraulic parameters influenced by local geomorphologic conditions. Seven levels are identified: *Catchment, River System, Zone, Macro-reach, Reach, Channel* and *Unit* (Table 4).

To both classification systems can also be added the *basin* level, used herein to designate an assemblage of linked catchments forming a unified drainage network (similar to a WR90 secondary drainage region).

Reaches can therefore be defined on a number of scales, depending on the purpose. For this study, representative reaches will be defined on the kilometres scale, as an aid in identifying potential variations in the hydraulic and hydrologic controls on the river.

Table 4: Reach hierarchical classification system.
After Heritage et al. (2000).

LEVEL	DESCRIPTION	TYPICAL SCALE
Catchment	All components of a river and its tributaries which contribute water and sediment to the channel.	km+
River System	Collection of zones incorporating the riparian margin from mouth to source.	km+
Zone	One or more segments with boundaries defined by major breaks in slope, often coincident with geological boundaries.	km+
Macro-Reach	One or more reaches with distinctive geological, hydrological, sedimentological and vegetational characteristics.	km+
Reach	Inter-related contiguous channels.	m – km
Channel	Combination of units.	m – km
Unit	A distinctive micro-habitat.	m

2.3.2 Representative reaches

A representative reach is a length of channel characterized by a particular channel pattern and morphology, resulting from a uniform set of local constraints on channel form (Rowntree and Wadeson, 1999). Examination of river cross-sections shows that the lower Renoster River consists primarily of a macro-channel with a single active channel. Bedrock features predominate, with the channel varying between straight and sinuous single-thread flow. Order changes (Figure 9) are insignificant in the lower Renoster River basin, occurring higher up in the catchments. Vegetation appears to be controlled by the presence of perennial pools (Figure 13), with abundant riparian forest present along much of the channel.

Within the lower Renoster River basin, four representative reaches can be identified (Table 5).

I. A relatively broad active channel filling a sinuous macro-channel (Figure 12B) within the superimposed river system. Banks are vertical and show signs of erosion and undercutting. This type is restricted to catchment C70D (Figure 3), immediately downstream of Koppies Dam. Local sinuosity of the macro-channel is 1.9. Riparian forest is present along the banks.
II. A terraced, sinuous macro-channel with an narrow incised active channel (Figure 12C) within the superimposed river system. Macro-channel banks are near vertical. This reach occupies the broad flat floodplain defined by catchment C70F, up to the confluence of the Heunigspruit. Local sinuosity of the macro-channel equals 1.8.

Riparian forest is present along the banks, although much of the floodplain has been converted to agricultural land.

III. A straight broad channel inside a narrow floodplain (Figure 12E) within the annular river system. Banks have a gentle slope. This type is predominate in catchment C70J, where the local sinuosity is 1.3. Riparian forest is present along the banks.

IV. A sinuous broad channel inside a broad floodplain (Figure 12J), corresponding to catchment C70K, with a local sinuosity of 1.7. Banks have a very gentle slope. Water hyacinth (Eichornia crassipes) is ubiquitous throughout the reach. Riparian forest is abundant along the banks. This reach is downstream of the last gauging station along the Renoster River.

The boundary between catchments C70J and C70K is marked by the river breaching a plunging quartzite anticline (Figure 12I) and cutting across a series of resistant quartzite layers. Once past the resistant structure the river becomes broader with a higher degree of sinuosity, displaying an upstream behavior and sinuosity similar to that reported by Tooth et al. (2004) for knickpoint controlled Highveld rivers. Sinuosity was also used to differentiate representative reaches. Leopold and Wolman (1957) defined the break between a straight and a meandering river as 1.5; by this criteria type II is distinct from types I,III and IV.

Table 5: Representative reaches.

PHOTO	TYPE	LOCATION	CATCH-MENT	COORDINATES	ACTIVE CHANNEL		MACRO-CHANNEL	
					Width	Height	Width	Height
A	I	R720	C70D	27.26°S 27.56°E	20	2	25	8
B	I	BRIDGE	C70F	27.27°S 27.53°E	15	2	20	8
C	II	N1	C70F	27.23°S 27.50°E	12	2	35	12
D	II	R721	C70F	27.24°S 27.32°E	11	2	30	9
E	III	WEIR	C70F	27.26°S 27.17°E	----	----	50	4
F	III	SPES BONA	C70J	27.12°S 27.11°E	----	----	60	7
G	III	R59	C70J	27.10°S 27.06°E	----	----	80	3
H	III	DRIFT	C70J	27.07°S 27.04°E	----	----	80	2
I	IV	R501	C70K	27.04°S 27.00°E	----	----	80	11
J	IV	MOUTH	C70K	26.98°S 26.92°E	----	----	>200	?

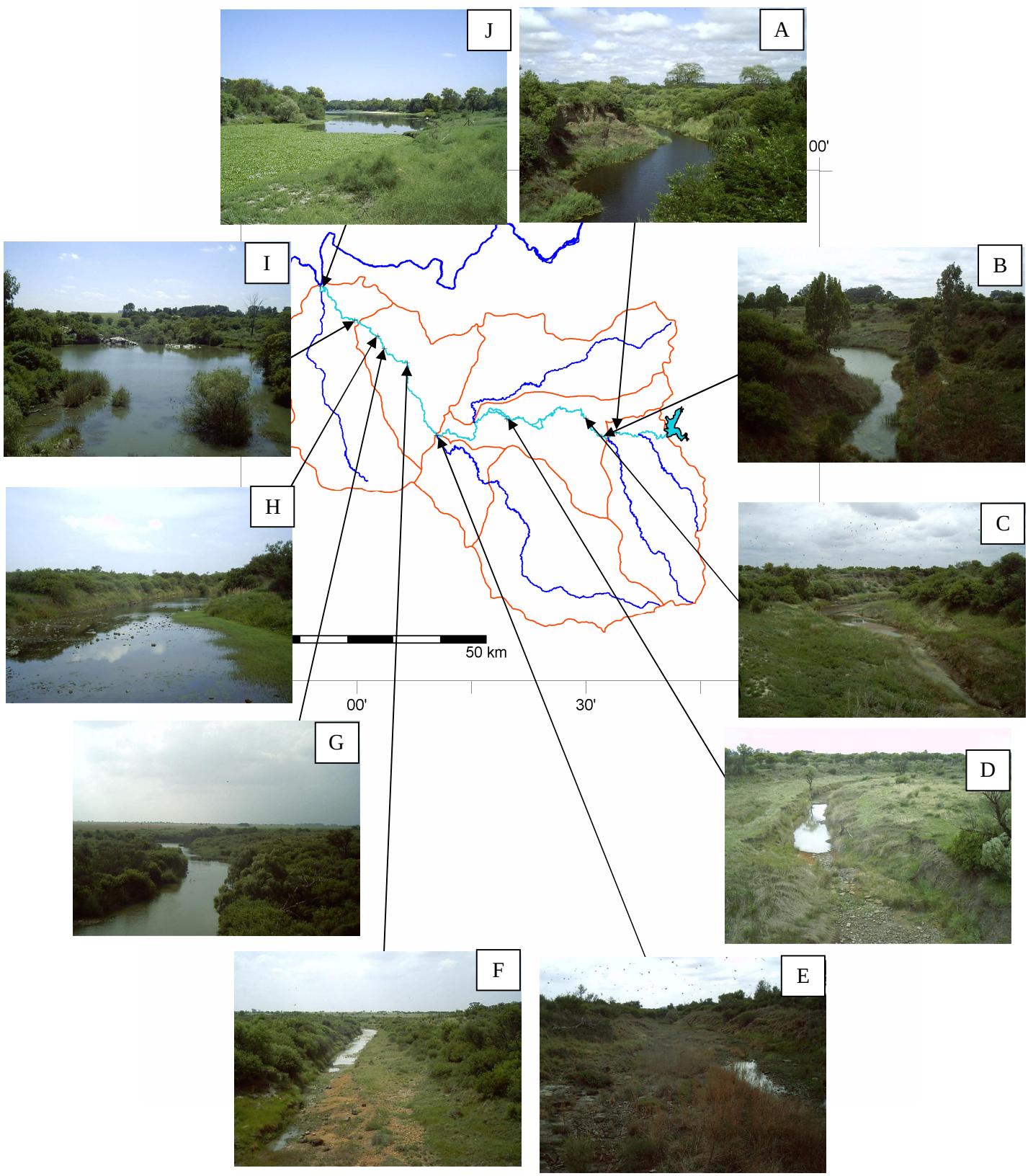


Figure 12: Representative reaches along the lower Renoster River.

3 HYDRAULIC MODEL

Hydraulic modeling was used to provide an estimate of potential short term water losses associated with discrete release events from the Koppies Dam into the lower Renoster River. Measured hydrographs provided an overall estimate of losses from selected events, and a Muskingum routing model provided an estimate of travel time from source to outlet. Kinematic wave routing was then implemented to model various flow regimes and their associated theoretical losses.

3.1 Water balance

The basic equation for a water balance within a catchment can be expressed as (after Shaw 1994):

$$Q = \Sigma I + P - E \pm T \pm \Delta S - O \quad (1)$$

where Q = river discharge, ΣI = sum of all channel inflows, P = precipitation, E = evapotranspiration, T = transmission loss, ΔS is the change in storage and O = outflow.

Hydrometric data can be used to quantify losses by comparing the inflow and outflow volumes of a channel reach. Input-output relationships for measured channel reaches can also be combined with simple flow routing schemes. Total storage is implicitly accounted for in the calibration of the routing parameters for the river channel, which is based on observed hydrographs (Birkhead and James, 2002). Variances in the water balance between the input and output hydrographs can therefore be related to changes in discharge between the hydrograph locations.

The total storage within a river can be further affected by anthropogenic effects, detention, lateral inflows and outflows, transmission losses, groundwater exchange and evapotranspiration. Inflow represents the main channel flow. Precipitation contributes to main channel flow through tributary flow and direct runoff. Total flow is reduced by evapotranspiration, and can be further modified by transmission flow out of or into local storage. By comparing the gauged outflow against the measured input the value of the various parameters can be estimated.

Flow reduction by infiltration to the bed, channel banks and the flood plain is grouped under the term transmission loss (Walters, 1990). Smakhtin and Watkins (1997) include the following as important components of transmission loss in South Africa:

- seepage areas where groundwater or channel bank soil water is subject to evaporation and transpiration loss;
- infiltration of low flows into the channel bed;
- bed losses to unconsolidated alluvial material;
- infiltration and extraction from bank storage.

Although the importance of transmission losses to the over-all water balance has been widely reported (see Lange, 2004, for a summary), the complex processes involved make it difficult to quantify.

McKenzie and Roth (1994) identified evaporation, transpiration, bed and bank flow as being the principle sources of water loss in the Orange and Vaal Rivers, although they considered transmission losses to be insignificant in comparison to evapotranspiration. Significant losses in ephemeral rivers can also occur during out-of-bank flow, where events that exceed the limits of the channel can infiltrate the alluvium of the flood plain and become exposed to evaporation and transpiration loss (Graf, 1988).

Irrigation releases from the Koppies Dam are routed through a separate canal system, and therefore have no direct influence on the release flow hydrographs or streamflow data. Some return flows to the Renoster may be present, but due to the high evapotranspiration rate return flows were regarded as insignificant and ignored for this study. Numerous small earth dams and detention sites are also present within the various catchments, which serve to further restrict return flows and may reduce runoff.

Detailed information on groundwater sources is not readily available. Existing boreholes appear to be intermittent and unreliable. Groundwater exploration in catchments C70G and C70H has identified deep fracture systems (> 100 metres below surface) in Karoo rocks as a potential groundwater source, although no sustainable source was located during drilling. Identified shallow aquifers have low groundwater potential (KLMCS, 2004).

The lower Renoster River is predominately a series of connected perennial pools, with a potentially significant storage capacity (Figure 13). The lack of identified shallow aquifers limits the potential recharge sources for the pools to runoff and interflow. Surface areas of the pools were measured from the 1:50000 digital topographic data sets, and an approximate volume was calculated assuming an average depth of 1.5 metres (Table 6). All models assume that the perennial pools are at maximum capacity, and will not affect downstream flow. If this condition is not met, flow will divert to detention storage until total capacity is reached. Riparian vegetation is also a potential source of transpiration loss, and its areal extent along each reach was estimated from the DEM and is included in Table 6.

In addition, an in-stream retention weir is located downstream of the confluence of the Heunigspruit and Renoster (Figure 14). This structure dates back to the early 1900's, and associated streamflow data are available for the period 1923 – 1947 (Gauging Station C7H001). The weir itself is a masonry structure approximately 30 metres in length and 5 metres in height, with a gross storage capacity of 285 000 m^3 (Alheit and Wiid, 2003). It was assumed for modeling purposes that the retention weir was at full capacity and would not affect flow.

Table 6: Perennial pool volumes and extent of riparian vegetation.

Catchment	**Pool Area (m^2)**	**Pool Volume (m^3)**	**Riparian Vegetation Area (m^2)**
C70K	866 204	1 299 306	1 098 000
C70J[1]	577 932	866 898	2 268 000
C70F	1 358 319	2 037 479	1 338 000
C70D	25 663	38 495	636 000
TOTAL	2 828 118	4 242 177	5 340 000
[1]Excludes retention weir.			

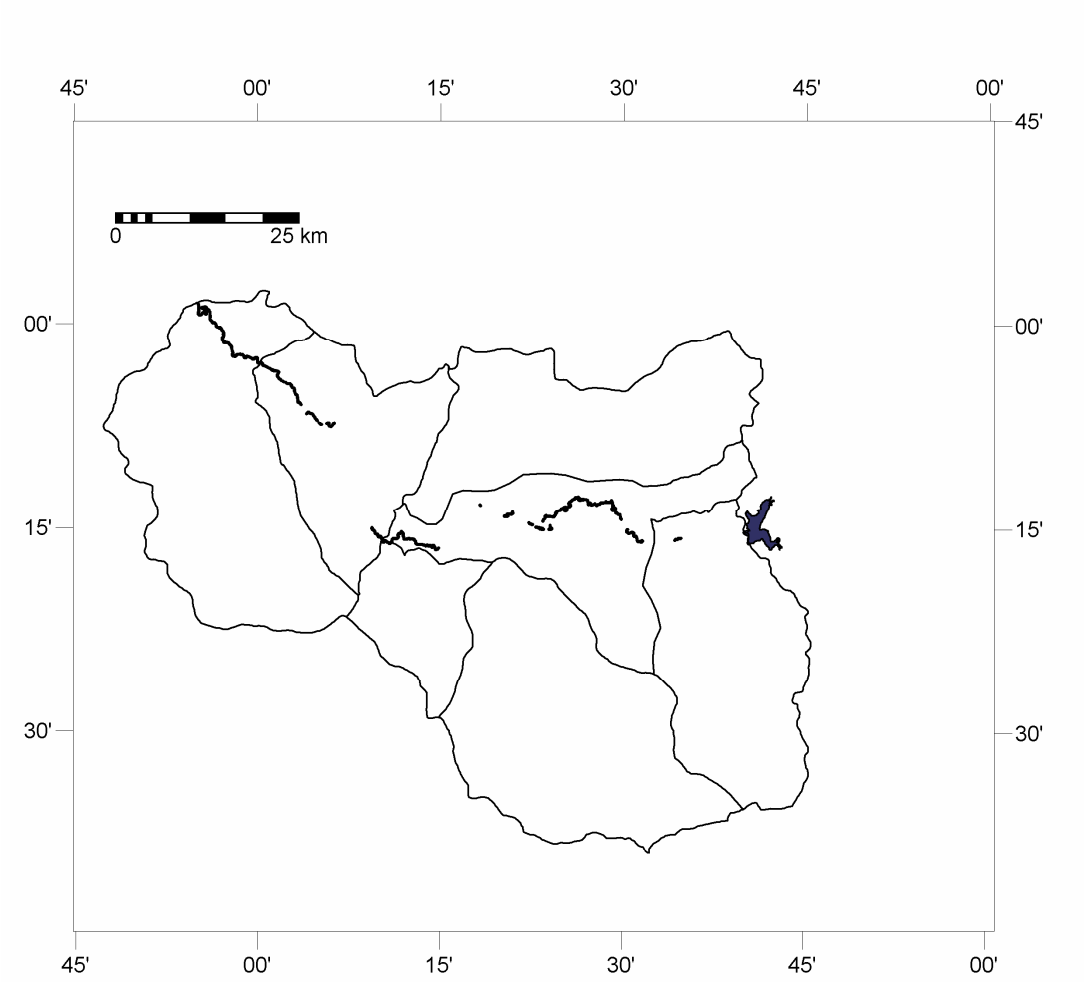


Figure 13: Perennial pools along the lower Renoster River.



Figure 14: Retention weir and Gauging Station C7H001.

3.2 Muskingum flow routing

Percentage flow losses were determined from the difference between the inflow and outflow volumes as derived from measured hydrographs. Muskingum routing was used to provide an estimate of travel time from the Koppies Dam to the confluence of the Renoster and Vaal Rivers.

3.2.1 Theory

Unsteady flow routing in open channels may be undertaken using a variety of methods. One of the simplest models in general use is the Muskingum-type approximation, although Lange (2004) suggests that outflow hydrographs can only be effectively estimated for relatively short confined reaches by the three-parameter Muskingum procedure. For Muskingum-type routing the flow conditions at two locations along a river reach are related using the continuity equation (Wilson, 1990):

$$dS/dT = I - O \quad (1)$$

where I = the inflow rate, O = the outflow rate and dS/dT is the rate of change of storage within the reach. The Muskingum method assumes that storage within the reach is dependent on the hydraulic characteristics of the channel section, expressed as:

$$S = K(xI + (1 - x)O) \quad (2)$$

where K is a function of the storage time within the reach and x is a weighting factor for a given river segment.

Equations (1) and (2) are then applied by expressing the continuity equation in finite difference form as:

$$(I_1 + I_2) / 2 - (O_1 + O_2) / 2 = (S_2 - S_1) / \Delta t \quad (3)$$

The change in storage within a river reach for the interval Δt can then be expressed as:

$$S_2 - S_1 = K\,(x(I_2 - I_1) + (1 - x)(O_2 - O_1) \quad (4)$$

When substituted into the finite difference form of the continuity equation this results in the standard Muskingum routing equation:

$$O_2 = C_0 I_2 + C_1 I_1 + C_2 O_1 \quad (5)$$

where the coefficients are derived from K, x and t:

$$C_0 = -(Kx - t/2)/(K - Kx + t/2),\ C_1 = (Kx + t/2)/(K - Kx + t/2),\ C_2 = (K - Kx - t/2)/(K - Kx + t/2) \quad (6)$$

Parameters K and x in a Muskingum model can be derived by graphical calibration using measured inflow and outflow discharge hydrographs. The factor x is selected so that the storage volume is the same whether the stage is rising or falling. For spillway discharges from a reservoir the factor x should be zero, because the reservoir stage and hence the storage are uniquely defined by the outflow. For uniform flow, x = 0.50, as both the outflow and the inflow are equal in weight. The value of x should therefore range between 0.00 to 0.50, with an average of 0.25 for river reaches. The factor K is the slope of the storage-weighted discharge relationship, and empirical analysis has shown that K is approximately equivalent to the time it takes for the center of mass of the flood wave to pass from the upstream end to the downstream end of the reach (Carter and Godfrey, 1960).

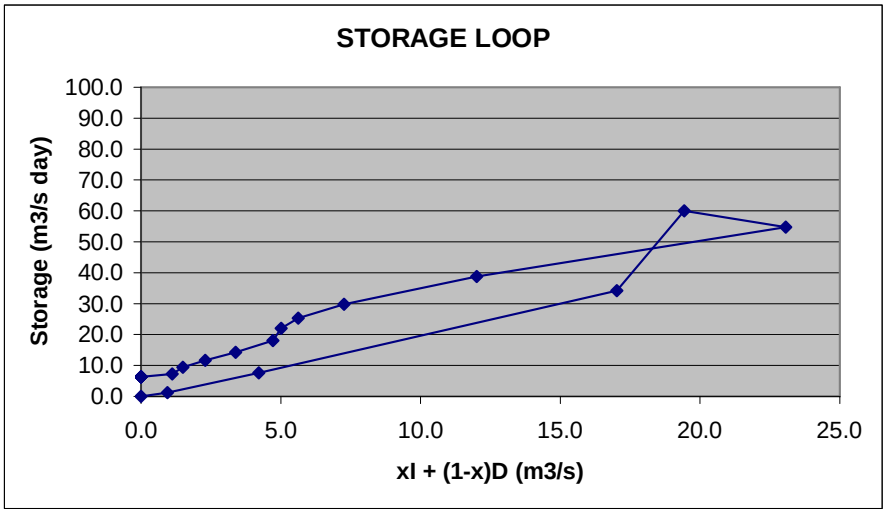
3.2.2 Muskingum routing hydrographs

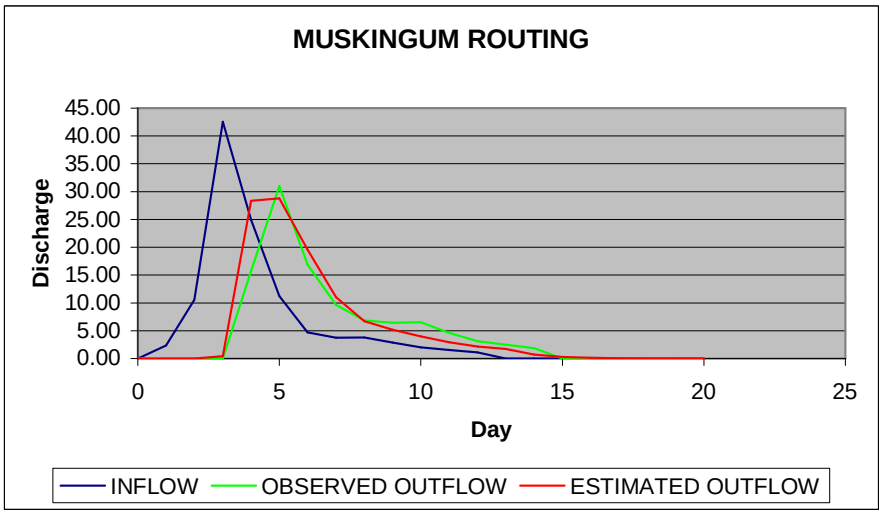
Complete daily streamflow (DWAF, 2004) and precipitation (Lynch, 2003) data are available for the period 1 September 1978 through 30 September 1989. For this period three hydrographs were isolated during which little or no precipitation was recorded in the lower Renoster River basin. These hydrographs were used to calibrate a Muskingum flood routing model between the Koppies Dam release point and the C7H006 Gauging Station, 126 km downstream. The percentage change between the upstream inflow hydrograph and the downstream observed hydrograph was then calculated as a lumped estimate of total loss within the reach.

Table 7: Muskingum flow routing results.

		Calibration		
Event	**Figure**	**K**	**x**	**% CHANGE**
January 1984	Figure 15	2.0	0.40	-4.9%
November 1987	Figure 16	1.6	0.40	-5.7%
January 1988	Figure 17	1.6	0.40	-5.1%
AVERAGE		1.7	0.40	-5.2%

Jan-84



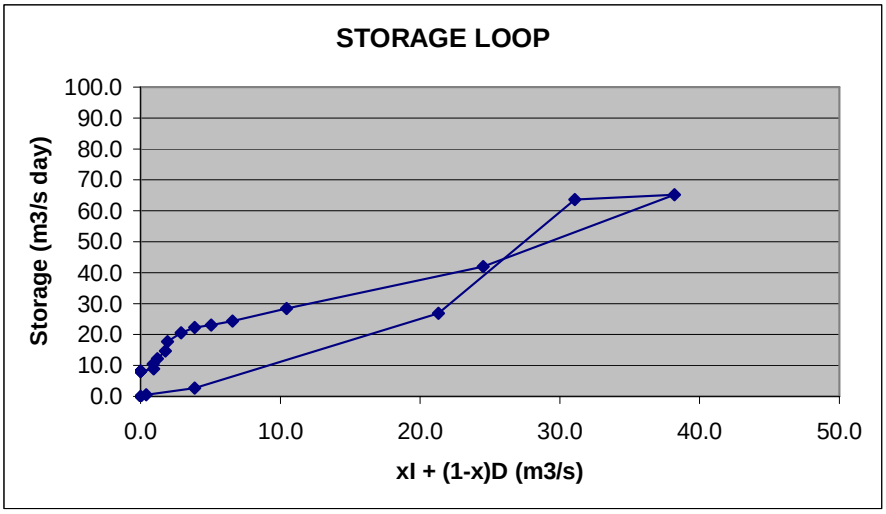


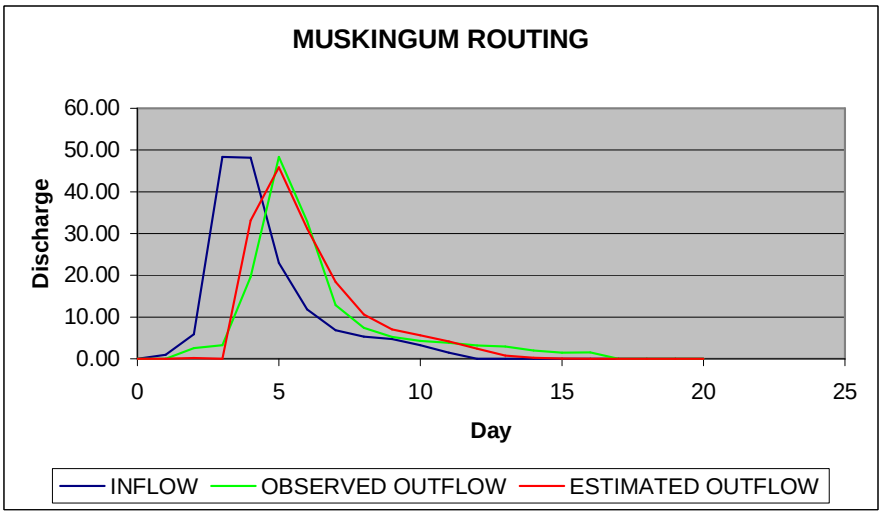
K	2
x	0.4
t	1

C0	-0.1765
C1	0.7647
C2	0.4118

Figure 15: Hydrograph and Muskingum routing Koppies release January 1984.

Nov-87



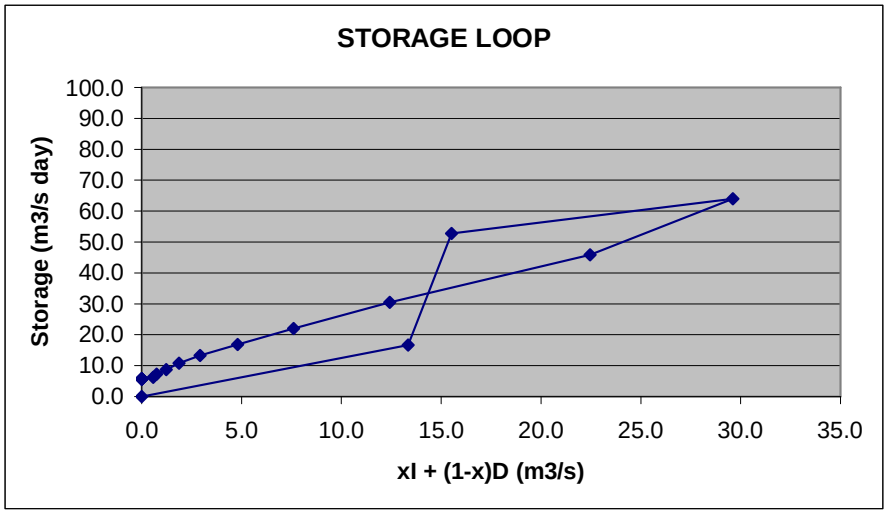


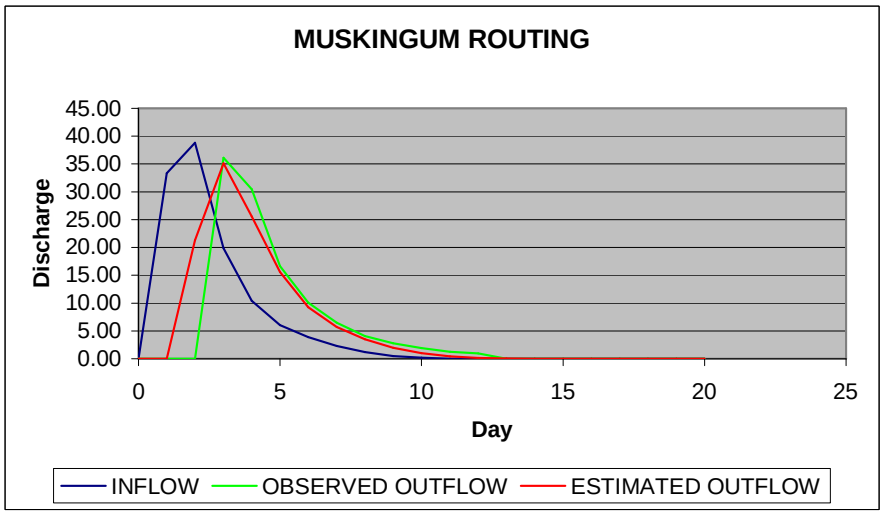
K	1.6
x	0.40
t	1

C0	-0.0959
C1	0.7808
C2	0.3151

Figure 16: Hydrographs and Muskingum routing Koppies release November 1987.

Jan-88





K	1.6
x	0.4
t	1

C0	-0.0959
C1	0.7808
C2	0.3151

Figure 17: Hydrographs and Muskingum routing Koppies release January 1988.

3.3 Kinematic wave routing

Kinematic wave routing was implemented in order to model release events from the Koppies Dam, based on losses derived from measured hydrographs. Such an approach permitted stage height, flow volumes and evaporation rates to be estimated for a variety of flow regimes.

3.3.1 Theory

The kinematic wave routing method solves the continuity equation along with a form of the momentum equation for a reach. Assuming no lateral inflow, the differential form of the continuity equation that is used is:

$$\delta A / \delta t + \delta Q / \delta x = 0 \quad (2)$$

where Q is discharge, x is the distance in the flow direction, A is the cross sectional area of flow and t is time. The kinematic approximation of the momentum equation assumes that the free surface is parallel to the channel:

$$S_0 = S_f \quad (3)$$

where S_0 is the bed slope representing the gravity force term and S_f is the friction force term. The maximum flow that can be conveyed through the reach is derived from the full-flow Manning's equation:

$$Q = 1/n\ AR^{2/3}\sqrt{S} \quad (4)$$

where Q = discharge, n is Manning's roughness coefficient, A is the cross-sectional area, R is the wetted perimeter, and S is interpreted as the slope of the channel. Manning's equation can then be rewritten as:

$$A = (nR^{2/3} / \sqrt{S_0})^{3/5}\ Q^{3/5} \quad (5)$$

The kinematic wave model requires one prescribed initial condition at t = 0 and one prescribed upstream condition for x at t > 0. Kinematic wave routing allows flow and area to vary both spatially and temporally within a reach. This can result in attenuated and delayed outflow hydrographs as inflow is routed through the channel. This form of routing cannot account for backwater effects, entrance/exit losses, flow reversal, or pressurized flow.

3.3.2 Manning's Coefficient

The implementation of kinematic wave routing requires an estimate of Manning's roughness coefficient, *n*, which represents the overall resistance to flow within the reach. The most important factors affecting the selection of an appropriate roughness coefficient are the type and size of the material that composes the channel bed, and the shape of the channel itself. Cowan (1956) developed a simplified procedure for evaluating the effects of the various components that contribute to total flow resistance, which can be expressed as:

$$n = (n_b + n_1 + n_2 + n_3 + n_4)m \quad (6)$$

where:

- n_b = a base value differentiating between stable and unstable channels;
- n_1 = a correction factor for base irregularities;
- n_2 = a value for variations in shape and size of the channel cross-section;
- n_3 = a value for obstructions;
- n_4 = a value for vegetation and flow conditions;
- m = a correction factor for channel meandering.

Arcement and Schneider (2000) provide a series of tables and photographs that can be used to estimate each component. Preliminary parameter values were assigned for each quaternary catchment based on the occurrence of representative reaches within the catchment (Table 8)

Table 8: Estimated Manning's roughness coefficients.

CATCHMENT	C70D	C70F	C70J	C70K
REACH	I	II	II/III	IV
n_b	0.020	0.020	0.010	0.020
n_1	0.005	0.002	0.001	0.001
n_2	0.002	0.001	0.001	0.002
n_3	0.004	0.020	0.002	0.001
n_4	0.025	0.020	0.030	0.020
m	1.300	1.100	1.000	1.200
Total n	0.073	0.069	0.044	0.053

3.3.3 Kinematic wave routing hydrographs

Kinematic wave routing was implemented using the U.S. Environmental Protection Agency Stormwater Management Model (Rossman, 2004). Individual channels were modeled as

trapezoidal channels with dimensions corresponding to measured cross-sections (Table 5) and the total length equal to the measured chainage. The simplified model consisted of four channels, three nodes and an outfall (Figure 18).

The inflow hydrographs identified in Section 3.2.2 were then routed through the model using a one hour time step. The estimated values for Manning's roughness coefficients for catchments C70D, C70F and C70J were varied for each simulation until a set of visual best fit hydrographs were obtained (Figure 19). Because catchment C70K is downstream of the gauging station no calibration was performed for this reach and its value was adjusted by the average change in value of the other reaches. The difference between the method of Arcement and Schneider (2000) compared to calibration using visual best fit hydrographs was on the order of 14% (Table 9).

Table 9: Calibrated Manning's roughness coefficients.

CATCHMENT	C70D	C70F	C70J	C70K
Estimated n from Arcement and Schneider (2000)	0.073	0.069	0.044	0.053
Calibrated n from hydrographs	0.064	0.057	0.038	0.045
Calibrated/Estimated	0.88	0.83	0.86	0.86

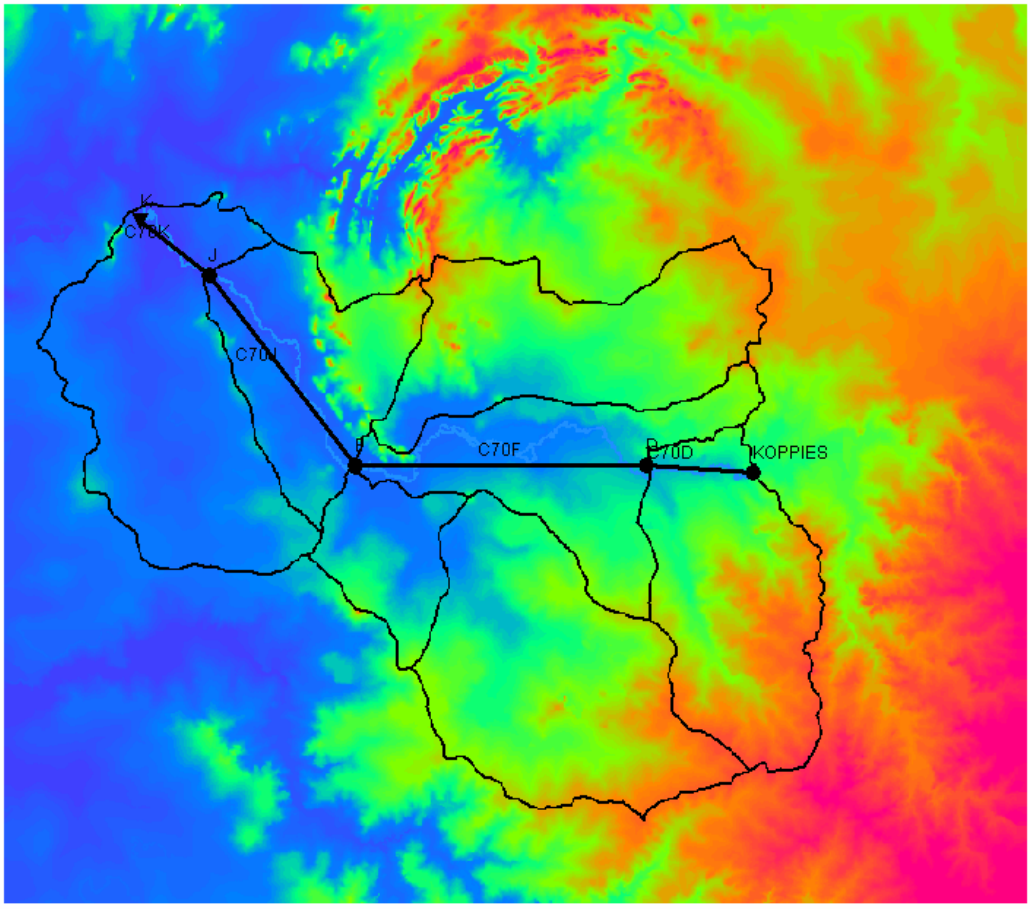
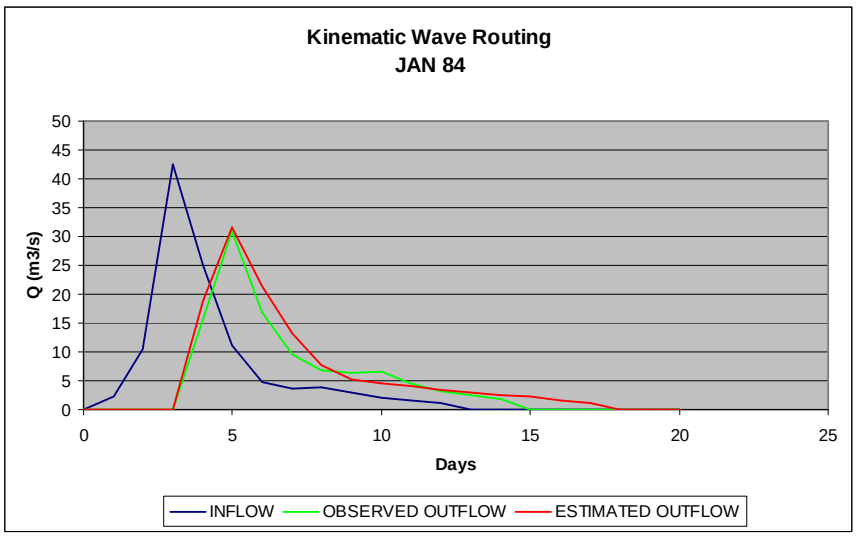
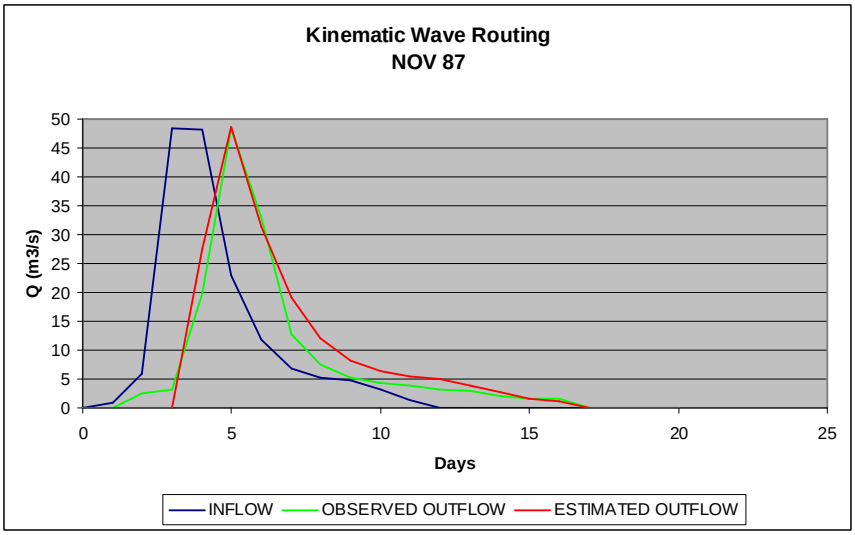


Figure 18: Kinematic wave routing model implementation.





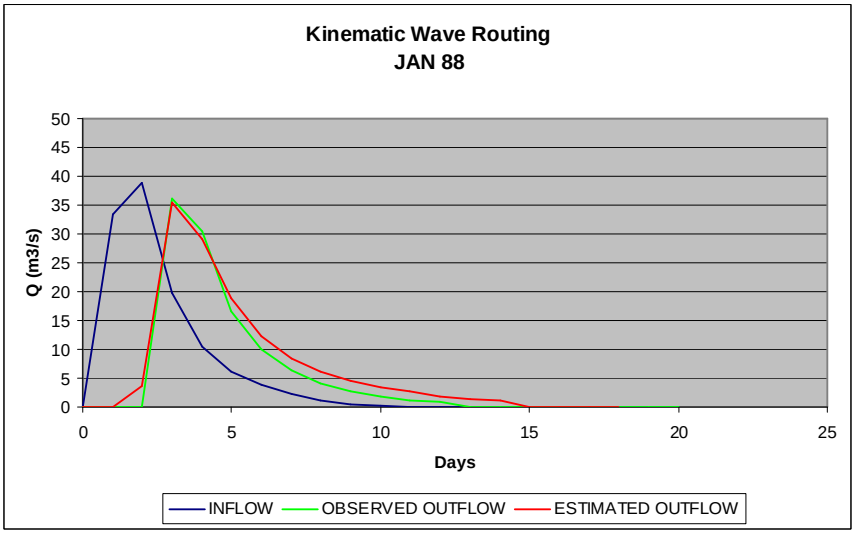


Figure 19: Kinematic wave hydrographs.

3.3.4 Loss calibration

The outputs of kinematic wave routing include velocity, total flow volumes, maximum stage and average stage per reach. From these the surface area can be calculated for the routed flows along each reach. Results for both the Muskingum routing and kinematic wave routing indicate a travel time from the Koppies Dam to gauging station C7H006 of ~41 hours for the hydrographs used. Travel time per catchment was allocated based on the total chainage of the three reaches (Table 10).

Table 10: Estimated travel time per catchment.

Catchment	Chainage (km)	Travel Time (hours)
C70D	21.2	7
C70F	66.9	22
C70J	37.8	12
TOTAL	126	41

If the channel geometry, average stage height and total flow volume are known then the flow surface area subject to evaporation can be determined. A theoretical evaporation loss rate for the lower Renoster River was estimated by using the average S-Pan value for November through January recorded at Koppies Dam (Midgley et al., 1994). This value was applied to the flow surface area for each reach, assuming an effective evaporation period per catchment based on travel time. Losses were applied sequentially to each channel within the model, and are expressed as a percentage of total input flow (Table 11).

Table 11: Estimated percent evaporation losses per reach.

	HYDROGRAPH			
REACH	JAN 84	NOV 87	JAN 88	AVG
C70D	0.5	0.5	0.6	0.5
C70F	1.7	1.5	1.7	1.6
C70J	1.8	1.5	1.7	1.7
TOTAL	4.1	3.4	4.0	3.8

Transpiration losses were estimated by using the average November through January S-Pan value applied to the area covered by the riparian vegetation along each reach, using a factor of 1.0 (Birkhead et al., 1997). Results from all simulations were consistently at or below 0.2% for estimated transpiration loss.

For the routed hydrographs precipitation and tributary inflows are nil, return flows can be discounted, and transpiration losses are ~ 0.2%. Estimated evaporation losses are slightly less than measured losses. Transmission losses were therefore of the order of 1%.

Additional out-of-bank losses can occur if the flow exceeds bank-full stage and dissipates through the surrounding flood plain. Kinematic routing was run on a variety of discharge levels based on the geometry of the macro-channel (Table 5), and it was determined that out-of-bank flow will occur if the discharge exceeds ~300 m^3/s (Figure 20), which represents less than 1% of the historical release flows (Figure 8).

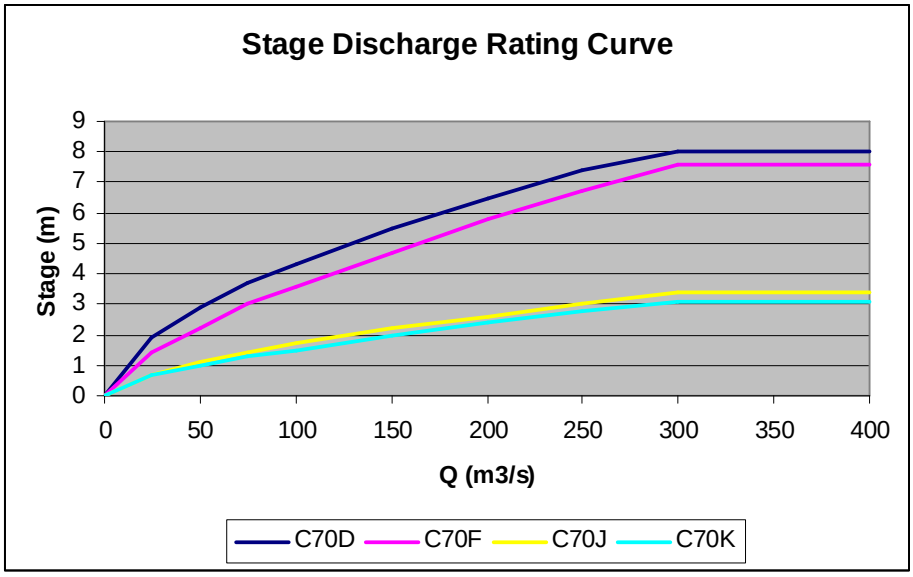


Figure 20: Stage/Discharge rating curve for the lower Renoster River macro-channel.

3.4 Theoretical losses

Based on the calibrated routing model a number of scenarios were run to determine the impact of various flow regimes on water loss for discrete events, assuming a constant lumped transmission loss of 1.0% and constant transpiration losses of 0.2%. Releases were simulated varying between 50 m^3/s and 300 m^3/s, for durations of 24, 48 and 72 hours, estimated over the hydrological year using average monthly evaporation rates for the lower Renoster River. Water surface areas and corresponding evaporation losses were estimated for each simulation. For all simulations it was assumed that perennial pools were in a full state. Losses were estimated for the channel extending from the release point at the Koppies Dam to Gauging Station C7H006. Loss estimates range from 3% to 17%, and are highest for lower, shorter duration discharges in the warmer summer months. Results are summarized in Table 12.

Table 12. Theoretical water losses as a percentage of total release.

	24 Hour Discharge Rate (m3/s)					
	50	100	150	200	250	300
Oct	13.0	9.4	8.5	7.5	6.9	6.6
Nov	15.8	12.3	11.1	9.8	9.0	8.5
Dec	17.2	13.3	11.9	10.6	9.6	9.2
Jan	16.9	13.2	11.8	10.4	9.5	9.1
Feb	13.9	10.9	9.8	8.7	7.9	7.6
Mar	12.8	10.0	9.0	8.0	7.3	7.0
Apr	9.6	7.6	6.9	6.1	5.6	5.4
May	7.5	6.0	5.5	4.9	4.5	4.4
Jun	6.1	4.9	4.5	4.0	3.8	3.6
Jul	6.6	5.3	4.8	4.4	4.1	3.9
Aug	9.1	7.2	6.5	5.8	5.4	5.1
Sep	12.3	9.6	8.7	7.7	7.1	6.8

	48 Hour Discharge Rate (m3/s)					
	50	100	150	200	250	300
Oct	11.4	8.9	8.0	7.1	6.6	6.3
Nov	11.7	9.2	8.2	7.3	6.8	6.4
Dec	12.6	9.9	8.9	7.9	7.3	6.9
Jan	12.5	9.8	8.8	7.8	7.2	6.8
Feb	10.3	8.1	7.3	6.5	6.0	5.8
Mar	9.5	7.5	6.8	6.0	5.6	5.3
Apr	7.2	5.8	5.2	4.7	4.4	4.2
May	5.7	4.6	4.2	3.8	3.6	3.5
Jun	4.7	3.8	3.5	3.2	3.0	2.9
Jul	5.1	4.1	3.8	3.5	3.3	3.1
Aug	6.8	5.5	5.0	4.5	4.2	4.0
Sep	9.2	7.2	6.5	5.8	5.4	5.2

	72 Hour Discharge Rate (m3/s)					
	50	100	150	200	250	300
Oct	9.3	7.2	6.6	6.0	5.6	5.4
Nov	9.6	7.4	6.8	6.2	5.8	5.5
Dec	10.3	7.9	7.3	6.6	6.2	5.9
Jan	10.2	7.8	7.2	6.5	6.1	5.8
Feb	8.5	6.5	6.0	5.5	5.2	5.0
Mar	7.8	6.1	5.6	5.1	4.8	4.6
Apr	6.0	4.7	4.4	4.0	3.8	3.7
May	4.8	3.9	3.6	3.3	3.2	3.1
Jun	4.0	3.2	3.0	2.8	2.7	2.6
Jul	4.3	3.5	3.2	3.0	2.9	2.8
Aug	5.7	4.5	4.2	3.9	3.7	3.5
Sep	7.5	5.9	5.4	5.0	4.7	4.5

4 HYDROLOGICAL MODEL

A Pitman monthly rainfall/runoff model was used to estimate potential water losses that might occur under long term constant flow conditions. The model was calibrated using monthly normalized rainfall and measured monthly naturalized streamflow data.

4.1 Pitman runoff model

The Pitman monthly rainfall-runoff model (Figure 21) is a deterministic lumped-parameter conceptual model (Singh, 1995) of medium complexity (Ye at al., 1997), developed specifically for hydrological regimes common to South Africa (Pitman, 1973). The model runs on a monthly time step.

The model uses eleven user-specified parameters to account for the processes involved in rainfall – runoff transformation (Table 13). ZMIN and ZMAX define respectively the minimum and maximum absorption rates of the catchment. Surface runoff calculations are based on a symmetrical triangular distribution of absorption rates. For any given rainfall rate, the area under the triangle defined by ZMIN and ZMAX represents the proportion of the catchment that contributes to surface runoff. Although regionally classified by Midgley et al. (1994) as a perennial system, the lower Renoster River basin response will vary between intermittent and perennial depending on local conditions due to the anthropogenic controls on river flow.

ST represents all subsurface storage within the catchment (Hughes, 2004). Runoff from storage is controlled by a non-linear relationship between runoff and storage through the parameter POW. At full storage the runoff rate is equivalent to FT, of which the portion GW is discharge from groundwater sources and lagged separately. Below SL no runoff occurs from subsurface storage. TL and GL represent runoff delays from surface and subsurface storage and are lagged separately using a Muskingum routing routine in order to simulate upper and lower soil moisture stores.

Evaporation is controlled by parameter R ($0 \leq R \leq 1$) in conjunction with potential evaporation values. Low values of R signify higher evaporation losses while higher values suggest less effective evaporation.

Other problems associated with the application of the Pitman model include the use of widely spaced rainfall data in a large catchment and the appropriateness of the conceptual model structure to runoff generation (Hughes, 1995).

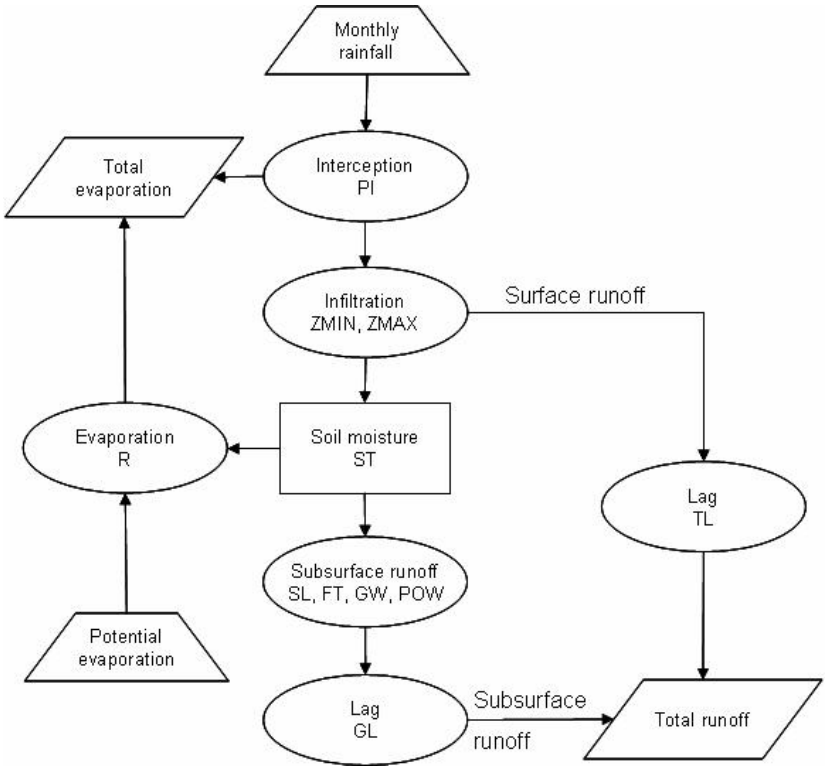


Figure 21: Pitman runoff model flow chart.

Table 13: Pitman model parameters.

PARAMETER	UNITS	DESCRIPTION
ZMIN	mm/month	Minimum catchment absorption rate
ZMAX	mm/month	Maximum catchment absorption rate
ST	mm	Subsurface storage
TL	month	Surface runoff lag
POW	----	Power of soil-moisture runoff equation
FT	mm/month	Runoff when ST is reached
GW	mm/month	Maximum groundwater runoff
GL	month	Soil moisture runoff lag
SL	mm	Soil moisture storage below which no runoff occurs
PI	mm	Interception storage
R	---	Evaporation – soil moisture relationship

4.1.2 Default Pitman model parameters

For the lower Renoster River Basin, Midgley et al. (1994) derived the following regionalized catchment model parameters (Table 14):

Table 14: Regionalised catchment model parameters.
After Midgley et al. (1994).

	C70D	C70E	C70F	C70G	C70H	C70J	C70K
POW	3.0	3.0	3.0	3.0	3.0	3.0	3.0
SL	0.0	0.0	0.0	0.0	0.0	0.0	0.0
ST	90	90	90	83	90	90	90
FT	7.0	7.0	7.0	0.5	7.0	2.0	2.0
GW	0.0	0.0	0.0	0	0.0	0.0	0.0
ZMIN	35	35	35	999	35	60	60
ZMAX	680	680	680	999	680	450	450
PI	1.5	1.5	1.5	1.5	1.5	1.5	1.5
TL	0.2	0.2	0.2	0.2	0.2	0.25	0.25
GL	0	0	0	0	0	0	0
R	0.5	0.5	0.5	0.5	0.5	0.5	0.5

4.2 WRSM2000 model

4.2.1 Model requirements

The WRSM2000 program (Pitman et al., 2001) is a software system that simulates a hydrological network based on the Pitman rainfall-runoff model. Components of the hydrological network are represented as modules within a linked system, driven by pre-defined monthly inflows and monthly rainfall time series data. The basic components of the system are:

- Runoff Module (RU): implements the Pitman rainfall-runoff model;
- Channel Module (CR): collects and redistributes inflows. The principal outflow route from a channel module represents the main river channel , and surplus flow is passed along this route after all demands are satisfied. Transmission losses can also be included.
- Reservoir Module (RV): represents a reservoir or equivalent storage. The reservoir module collects inflows and distributes outflows in a manner similar to a channel module. The one essential difference is the effect of storage, which requires that the reservoir be filled before outflow can take place;

- Route: a loss-free river reach connecting various modules. Gauging Stations containing data about historically observed flows can be associated with a route, and pre-defined flows can be used as inputs into the network.

Associated data required for the network are:

- Catchment details: total area, MAP, monthly pan evaporation data and pan factors, and Pitman model parameters;
- Rain files: monthly rainfall time series expressed as percentages of MAP for a catchment;
- Reservoir capacity and surface area.

4.2.2 Model implementation

The lower Renoster River basin was modeled as a semi-distributed implementation of the Pitman model using a series of linked catchments connected by channel reaches (Figure 22).

Rainfall-runoff was modeled using the Pitman model within each catchment. The influence of the perennial pools was modeled as a series of detention storage elements within the applicable channel reaches, and subject to evaporation losses.

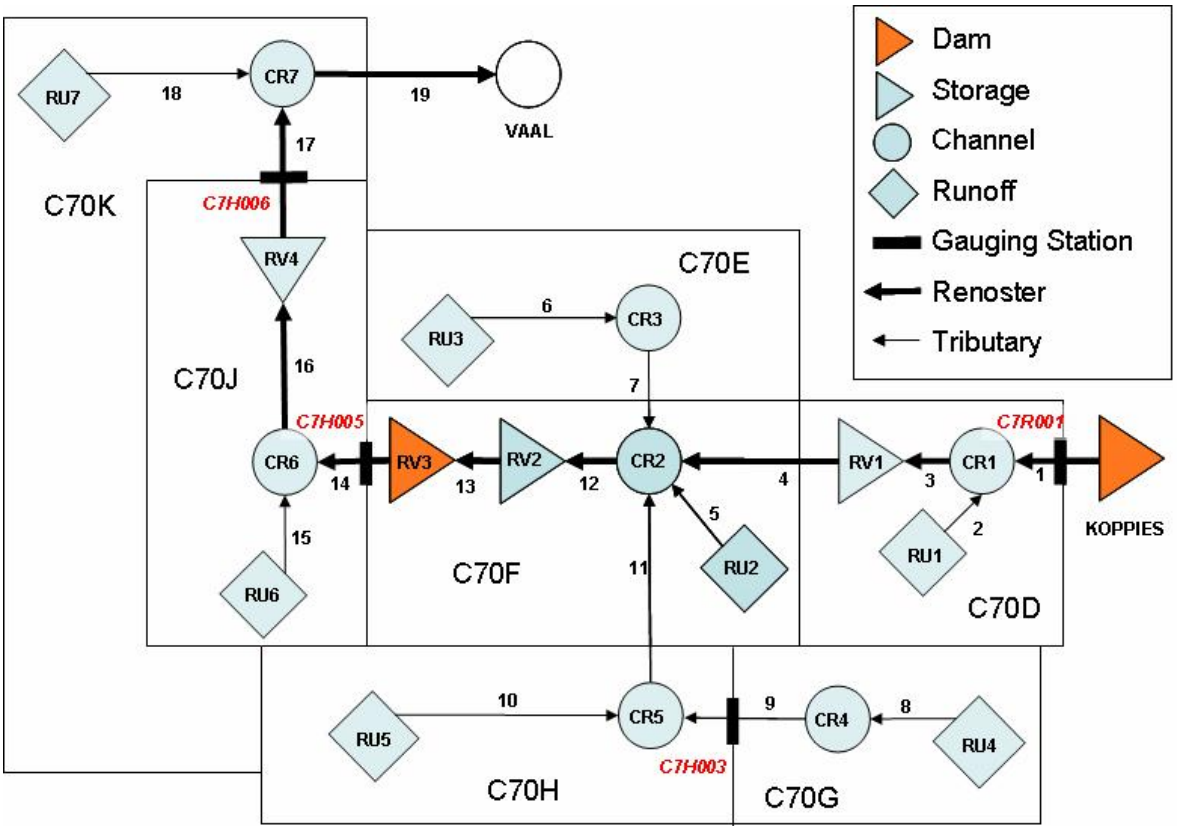


Figure 22: Lower Renoster River basin model network.

4.2.3 Calibration

Within the lower Renoster River basin inflow is provided by monthly dam release volumes from Gauging Station C7R001. Outflow is derived from monthly naturalized streamflow data for Gauging Station C7H006. Some intermediate data are also available for C7H005, and catchment C70G can be modeled separately using streamflow data available from gauge CH7003.

Two performance measures were used to manually calibrate the Pitman model parameter set for a monthly time step:

- Summary Statistics: Mean Annual Runoff, Standard Deviation and Seasonal Index. Midgley et al. (1994) recommend that calibration meet the following guidelines:

    - Error in Mean Annual Runoff (MAR). < 4%
    - Error in Standard Deviation: < 6%
    - Error in Seasonal Index: < 8%

- Efficiency:

$$E = 1 - \mu^2_e / \sigma^2_q \quad (7)$$

where μ^2_e is the second moment of the residuals and σ^2_q is the variance of the observed discharges. A value of unity therefore indicates a perfect correlation. Efficiency is indicative of the model's ability to explain the variance of observed streamflow and is biased toward higher flows, penalizing larger absolute discrepancies more than lower ones (Kokkonen and Jakeman, 2001). Such a performance statistic is more suited to the problem at hand, in that interest is focused on modeling relatively larger scale streamflow and variances.

4.4 Model results

4.4.1 Parameter set

Using the calibration parameters recommended by Midgley at al. (1994) (Table 14 above) resulted in a simulation that underestimated water losses. McKenzie and Craig (2000) reported similar results from their investigation of evaporation losses for the Orange River, which they attributed to underestimation of evaporation factors.

In order to compensate for this effect, the evaporation efficiency in the Pitman runoff model was maximized by decreasing the R parameter to zero. Empirical adjustments for each catchment were also required for infiltration and loss, resulting in a model that further minimized the influence of groundwater flow. The final parameter set (Table 15) provided a reasonable model when calibrated against streamflow gauging data (Table 16). Graphic results of the calibration process are displayed in Figures 23 and 24.

Table 15: Model parameter set.

	C70D	C70E	C70F	C70G	C70H	C70J	C70K
POW	2.5	2.5	2.5	4.5	2.5	2.5	2.5
SL	0.0	0.0	0.0	0	0.0	0.0	0.0
ST	140	140	140	120	140	140	140
FT	10	10	10	10	10	10	10
GW	0.0	0.0	0.0	0	0.0	0.0	0.0
ZMIN	200	200	200	600	200	200	200
ZMAX	800	800	800	800	800	800	800
PI	1.5	1.5	1.5	1.5	1.5	1.5	1.5
TL	0.2	0.2	0.2	0.2	0.2	0.2	0.2
GL	0	0	0	0	0	0	0
R	0	0	0	0	0	0	0

Table 16: Simulation summary statistics (Route 17 output).

	OBSERVED	SIMULATED
MAR	107.4	107.8
MEAN (LOG)	1.85	1.87
STANDARD DEVIATION	110.6	113.9
SEASONAL INDEX	35.3	33.1
EFFICIENCY	----	0.86

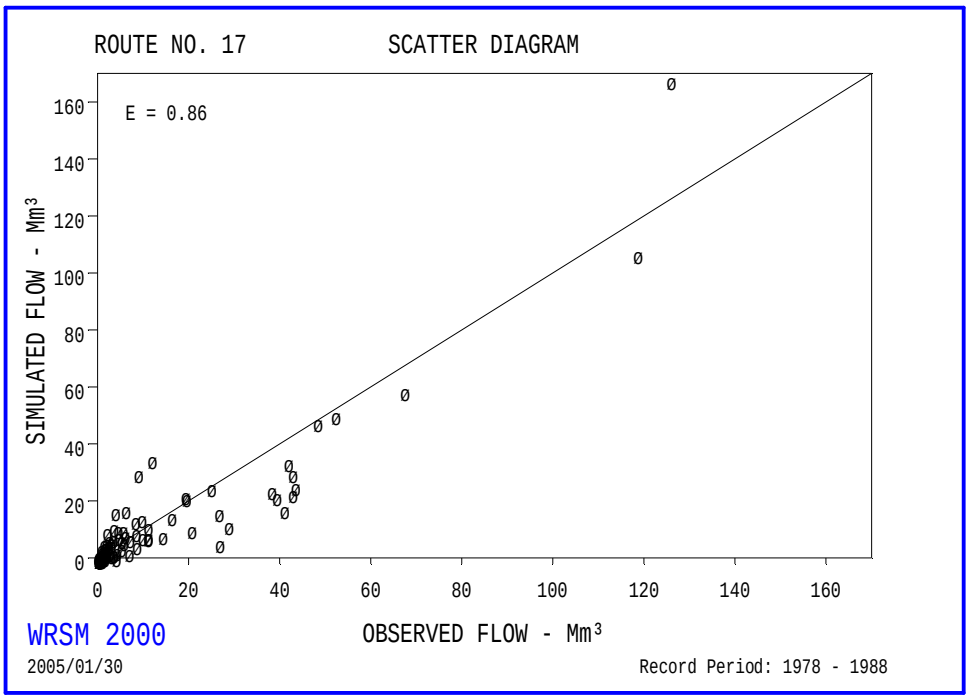


Figure 23: Calibration of the basin model – monthly simulated and observed flows.

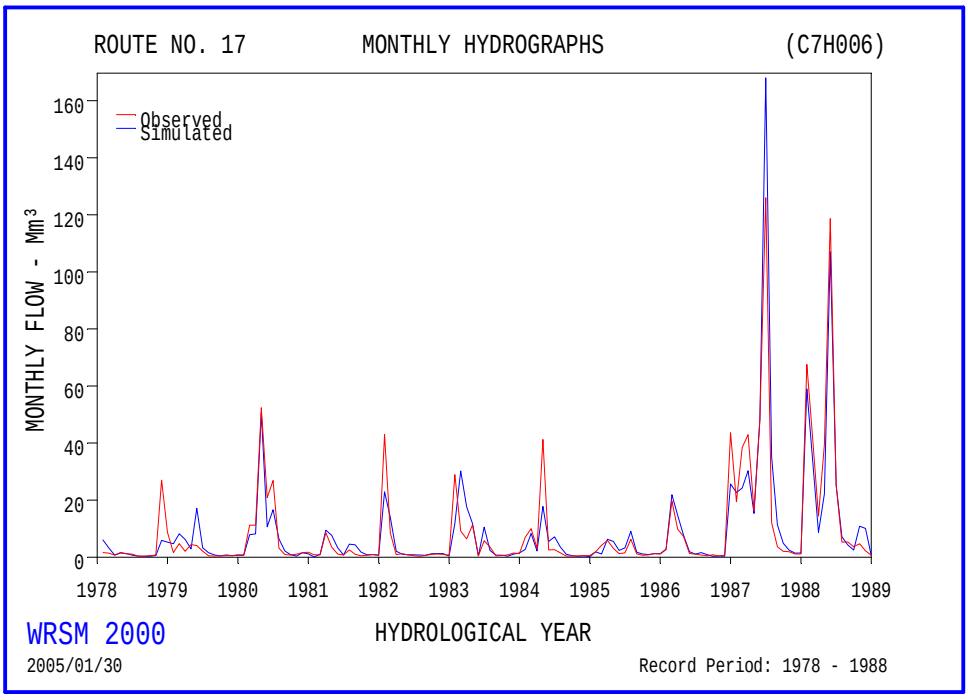


Figure 24: Calibrated monthly hydrograph.

4.4.2 Theoretical losses

The Pitman model is based on normalized monthly flow conditions. Potential water losses are estimated from the calibrated model by changing the boundary conditions of the simulation. Precipitation was set to zero, and the release of a fixed volume of water was simulated.

Water losses from the discharge point at Koppies Dam to Gauging Station C7H006 (corresponding to RQ17) ranged from ~10% in July to ~40% in January (Figure 25) for the hydrological month.

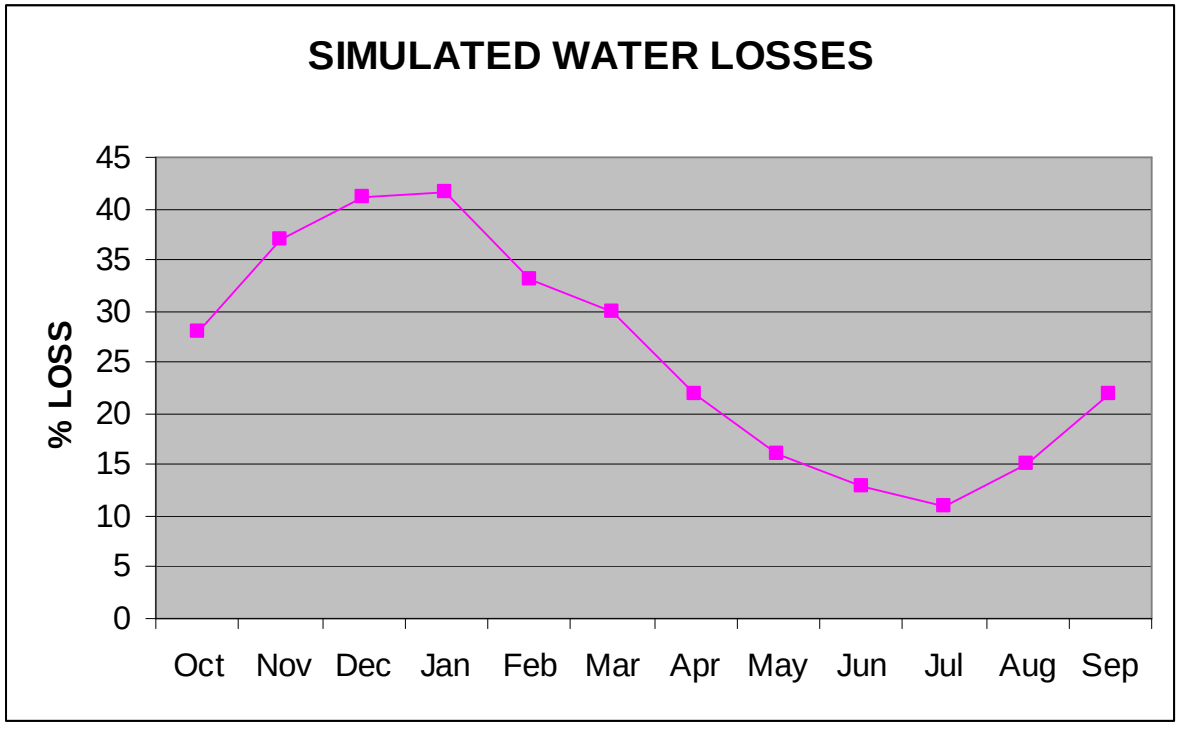


Figure 25: Simulated water loss in the lower Renoster River.

5 SUMMARY

In order to determine the potential loss of water released through the lower Renoster River a discrete hydraulic model and a longer-term hydrological model were developed. After calibration, the models were used to simulate potential losses within the system.

Based on the results obtained in this study, discrete flow losses from individual flood events along the lower Renoster River can vary between 3% and 17%. For a long term constant flow regime, losses can be expected to range between 10% and 40%. The principal cause of flow losses is evaporation, which is in agreement with the findings of McKenzie and Craig (2000) for the Orange and Vaal Rivers.

Muskingum flow routing and kinematic wave routing were used to calibrate a model for discrete flow events. The variation in loss for discrete flow events was modeled primarily as a function of the change in surface area exposed to evaporation Losses, expressed as a percentage of total volume released, are minimized by using higher flow rates over the maximum period possible. Releases however need to be limited to less than 300 m^3/s, in order to prevent out-of-bank flow and subsequent associated losses. Transmission losses for discrete events were modeled as a constant 1% loss across the range of flow conditions investigated. Lange (2004) has however reported that transmission losses in the Kuiseb River in Namibia can become significant when a discharge threshold limit is exceeded. Although transpiration losses have been shown to be significant in the more humid regions of South Africa (Birkhead et al., 1997), their impact in the more arid Free State region appears to be insignificant along the lower Renoster River.

A Pitman monthly rainfall-runoff model was used to model longer term historical streamflow data. In order to implement the rainfall-runoff model precipitation data were also utilized in order to estimate the contribution of rainfall to monthly gauged streamflow data. The recommended WR90 parameter set (Midgley et al., 1994) underestimated the influence of evaporation, and the evaporation – soil moisture coefficient was adjusted accordingly. The influence of ground water was also minimized in order to meet the calibration criteria of the model.

All simulations assumed that the perennial pools and the retention weir were at full capacity and would not affect flow. If this is not the case then considerable flow detention will occur, on the order of 2.8×10^6 m^3 for the pools and 0.3×10^6 m^3 for the retention weir.

For eighty years flow in the lower Renoster River has been artificially controlled. Within that time period the river has adjusted itself to the imposed anthropogenic flow regime. Water

losses within this regime can be minimized by using a high discharge rate to a maximum of 300 m^3/s, combined with larger volumetric releases. Evaporation losses can be significant, and release strategies will need to take this into consideration.

REFERENCES

Alheit W, Wiid G (2003). Results of prefeasibility environmental and water investigations for Voorspoed Mine. Unpublished report, Murray & Roberts. Project Number 181-009, Johannesburg.

Arcement GJ, Schneider VR (2000).Guide for selecting Manning's roughness coefficients for natural channels and flood plains. U.S. Geological Survey Water-supply Paper 2339. U.S. Government Printing Office, Washington D.C.

Birkhead AL, James CS, Olbrich BW. 1997. Developing an integrated approach to predicting water use by riparian vegetation. Water Research Commission Report No. 474/1/97, Pretoria.

Birkhead AL, James CS (2002). Muskingum river routing with dynamic bank storage. Journal of Hydrology 264,113–132.

Bootsman CS, Reimold WU (2001). First results of a geomorphological study of the Morokweng and Vredefort impact structures in South Africa. In: Holland P, Stephenson F, Wearing A (eds.), *2001, Geography – a Spatial Odyssey*. Brebner Print, New Zealand.

Carter RW, Godfrey RG (1960). Storage and flood routing. U.S. Geological Survey Water-supply Paper 1543-B. U.S. Government Printing Office, Washington D.C.

Chief Directorate, Surveys and Mapping (1994). Mowbray, South Africa. http://www.nsif.org.za/sm_topo.htm.

Cowen WL (1956). Estimating hydraulic roughness coefficients. Agricultural Engineering. 37/7.

DWAF (2004). Retrieved 1 December 2004 from WWW site http://www.dwaf.gov.za/hydrology/cgi-bin/his/cgihis.exe/station, Department of Water Affairs and Forestry, Pretoria.

Gibson RL, Kisters AFM, Lana C, Reimold WU (2002). Archean crustal structure in the Kaapvaal craton, South Africa – evidence from the Vredefort Dome. Earth and Planetary Science Letters.

Graf WL (1988). Fluvial Processes in Dryland Rivers. Springer-Verlag, Berlin.

Heritage GL, Broadhurst LJ, van Niekerk AW, Rogers KH, Moon BP (2000). The definition and characterization of representative reaches for river management. Water Research Commission Report No. 376/2/00, Pretoria.

Hughes DA (1995). Monthly rainfall-runoff models applied to arid and semiarid catchments for water resource estimation purposes. Hydrological Science Journal 40/6.

Hughes DA (2004). Incorporating groundwater recharge and discharge functions into an existing monthly rainfall-runoff model. Hydrological Sciences Journal 49/2.

KLMCS (2004). KLM Groundwater Consulting Services. Personnel communication. Johannesburg, South Africa.

Knighton D (1998). Fluvial Forms and Processes. Arnold Publishers, London.

Kokkonen TS, Jakeman AJ (2001). A comparison of metric and conceptual approaches to rainfall-runoff modeling and its implications. Water Resources Research 37/9.

Lange J (2004). Dynamics of transmission losses in a large arid stream. Journal of Hydrology. xx 1-15.

Leopold LB, Wolman G (1957). River channel patterns: braided, meandering and straight. U.S. Geological Survey Professional Paper 282-B. US Government Printing Office, Washington D.C.

Lerner DN (2003). Surface water – groundwater interactions in the context of groundwater resources. In:. Xu Y and Beekman (eds.). *Groundwater Recharge Estimation in Southern Africa*. UNESCO IHP Series No. 94, Paris.

Low B, Rebelo T (1996). Vegetation of South Africa, Lesotho and Swaziland. Department of Environmental Affairs and Tourism, Pretoria.

Lynch, SD (2003) Development of a raster database of annual, monthly, and daily rainfall for Southern Africa. Water Research Commission Report No. 1156/1/03, Pretoria. In Press.

McKenzie RS, Craig AR (2000). Evaporation losses from the Orange River using hydraulic modeling. Journal of Hydrology 241, 62-69.

Midgley DC, Pitman WV, Middleton BJ (1994). Surface water resources of South Africa. Volumes I - II. Water Research Commission Report No. 298/2.1/94, Pretoria.

McKenzie RS, Roth C (1994). The evaluation of river losses from the Orange River downstream of the PK Le Roux Dam. Water Research Commission Report No. 510/1/94, Pretoria.

Pitman WV (1973). A mathematical model for generating monthly river flow from hydrometeorological data in South Africa. Hydrological Research Unit Report No. 2/73, University of the Witwatersrand, Johannesburg.

Pitman WV, Kaakebeeke JP, Bailey AK (2001). WRSM2000 Water Resources Simulation Model for Windows. Compiled by Stewart Scott Consulting Engineers. Department of Water Affairs and Forestry, Pretoria.

River Health Program (2003). State-of-Rivers Report, Free State Region River Systems. Department of Water Affairs and Forestry, Pretoria.

Rossman, LA (2004). Stormwater Management Model handbook, version 5.0. U.S. Environmental Protection Agency, Cincinnati.

Rowntree KM, du Plessis AJE (2003). Geomorphological research for the conservation and management of Southern African rivers. Volume 1: geomorphological impacts of river regulation. Water Research Commission Report No. 849/1/03, Pretoria.

Rowntree KM, Wadeson RA (1999). A hierarchical geomorphological model for the classification of selected South African rivers. Water Research Commission Report No. 497/1/99, Pretoria.

Shaw EM (1994). Hydrology in Practice. 3rd Edition, Nelson Thornes Ltd. UK.

Singh, VP (1995). Computer Models of Watershed Hydrology. Water Resources Publications, USA.

Smakhtin VY, Watkins DA (1997). Low flow estimation in South Africa. Water Research Commission Report No. 494/1/97, Pretoria.

Tooth S, Brandt D, Hancox PJ, McCarthy TS (2004). Geological controls on alluvial behavior: a comparative study of three rivers on the South African Highveld. Journal of African Earth Sciences 38.

Turton AR, Meissner R, Mampane PM, Seremo O (2004). A hydropolitical history of South Africa's international river basins. Water Research Commission Report No. 1220/1/04, Pretoria.

Van Westen C, Farifteh J (2002). ILWIS for Windows user's guide. International Institute for Aerospace Survey and Earth Sciences. Netherlands.

Walters MO (1990). Transmission losses in arid regions. Journal of Hydraulic Engineering, 116/1.

Wilson EM (1990). Engineering Hydrology. Palgrave Macmillian, New York.

Ye W, Bates BC, Viney NR, Sivapalan M, Jakeman AJ (1997). Performance of conceptual rainfall-runoff models in low-yielding ephemeral catchments. Water Resources Research 33/1.

Xu Y, Titus R, Holness SD, Zhang J, van Tonder GJ (2002). A hydro-geomorphological approach to quantification of groundwater discharge to streams in South Africa. Water SA 28/4.